Mon. Not. R. Astron. Soc. **000**, 000–000 (0000) Printed 2nd February 2008 (MN LaTeX style file v2.2)

arXiv:astro-ph/0401273v1 14 Jan 2004

Cepheid calibration of type Ia Supernovae and the Hubble constant

G. Altavilla[1,2]⋆, G. Fiorentino[3], M. Marconi[3], I. Musella[3], E. Cappellaro[3],
R. Barbon[2], S. Benetti[1], A. Pastorello[1,2], M. Riello[1,2], M. Turatto[1], L. Zampieri[1]
[1] *INAF - Padova Astronomical Observatory, vicolo dell'Osservatorio 5, I-35122 Padova, Italy*
[2] *Department of Astronomy, Padova University, Vicolo dell'Osservatorio 2, I-35122 Padova, Italy*
[3] *INAF - Capodimonte Astronomical Observatory, Via Moiariello 16, I-80131 Napoli, Italy*

Received ....; accepted ....

ABSTRACT

We investigate how a different calibration of the Cepheid Period-Luminosity (PL) relation taking into account the metallicity corrections, affects the absolute magnitude calibration of Supernovae (SNe) Ia and, in turn, the determination of the Hubble constant H_0. We exploit SN Ia light curves from literature and previously unpublished data, to build the $M_B - \Delta m_{15}(B)$ relation and we calibrate the zero point by means of 9 type Ia SNe with Cepheid measured distances. This relation was then used to build the Hubble diagram and in turn to derive H_0. In the attempt to correct for the host galaxy extinction, we found that the data seems to suggest a value for the total to selective absorption ratio, $R_B = 3.5$, which is smaller than the standard value for our own Galaxy $R_B = 4.315$.

Depending on different metallicity corrections for the Cepheids P-L relation, values of R_B and SN sample selection criteria, we found that the values of the Hubble constant H_0 is in the range 68–74 $\mathrm{km\,s^{-1}\,Mpc^{-1}}$, with associated uncertainties of the order of 10%.

Unpublished photometry is also presented for 18 SNe of our sample (1991S, 1991T, 1992A, 1992K, 1993H, 1993L, 1994D, 1994M, 1994ae, 1995D, 1995ac, 1995bd, 1996bo, 1997bp, 1997br, 1999aa, 1999dk, 2000cx), which are the results of a long standing effort for supernova monitoring at ESO - La Silla and Asiago Observatories.

Key words: supernovae: general – supernovae: calibration – supernovae: individual: 1991S, 1991T, 1992A, 1992K, 1993H, 1993L, 1994D, 1994M, 1994ae, 1995D, 1995ac, 1995bd, 1996bo, 1997bp, 1997br, 1999aa, 1999dk, 2000cx – supernovae: Hubble constant

1 INTRODUCTION

Type Ia supernovae are probably the most accurate distance indicators on cosmological scales. An important limitation is that, since SNe are relatively rare events, they cannot be used to measure the distance of pre-selected individual galaxies. On the other side they are invaluable tools to measure global properties of our Universe, like the Hubble constant H_0 (e.g. Rust 1974; Hamuy et al. 1996a; Tripp & Branch 1999; Freedman et al. 2001), the cosmological parameters q_0, Ω_m, Ω_Λ (e.g. Schmidt et al. 1998; Perlmutter et al. 1999; Riess et al. 1998), and also the peculiar velocity field (Riess et al. 1997). This explains the continuous efforts spent to refine the absolute calibration of SNe Ia.

Three main issues need to be addressed for a proper calibration of SNe Ia, namely the direct calibration of individual events through primary distance indicators, the determination of the relation between light curve shape and absolute magnitude and the extinction estimate, in particular that due to the host galaxy dust. This process is complicated by the fact that these three items have a deep interplay. This means that it is not easy to predict how the effect of a new finding on one ingredient propagates to the final result. Indeed, different assumptions in the calibration chain may

---

⋆ E-mail: altavilla@pd.astro.it

explain why different authors, using the same data, obtain different results (Leibundgut 2000).

The purpose of this work is to investigate how new calibrations of the Cepheids absolute magnitude, discussed in §2.4, propagate through the calibration of SNe Ia on the determination of H_0. In this work we do not rely on published values of SN light curve parameters (in particular maximum magnitudes and decline rates), but we made our own independent estimates. To this aim we exploited the archive of SN Ia light curves which has been collected at the Padova Observatory. Besides all relevant data published in the literature (with a major contribution given by Hamuy et al. 1996b and Riess et al. 1999), the archive includes also the results of a long standing effort for supernova monitoring at ESO and Asiago Observatories (Turatto 2000). The unpublished data are reported in Appendix A.
After rejecting objects with incomplete photometric coverage we retained a sample of 78 SNe Ia (see Appendix B).

The plan of the paper is the following: in §2 we discuss the SNe Ia inhomogeneity, the properties of their light curves and the calibration of the absolute magnitude at maximum. In particular we address the problem of the host galaxy absorption and the effect of the metal content on the Cepheid distance scale. In §3 we show how different assumptions on the peak magnitude calibration and different metallicity corrections on the Cepheid PL relation affect the Hubble constant. Conclusions are drawn in §4.

2 SNe Ia CALIBRATION

Contrary to early claims, the absolute magnitude of SNe Ia at maximum (M_{max}) is not constant but it ranges over 2–2.5 mag. However a correlation between M_{max} and the shape of the light curve has been suggested which allows to recover SNe Ia as accurate distance indicators. This was first proposed almost thirty years ago (Barbon, Ciatti & Rosino 1973; Rust 1974; Pskovskii 1977) but, because of the large photometric errors of photographic photometry and the contamination of the early sample from other SN types (SNe Ib/c in particular), remained debated until a few years ago (Sandage & Tammann 1993). Eventually, the improved accuracy obtained with CCD photometry definitively proved that M_{max} is brighter in SNe Ia with a slower luminosity decline (Phillips 1993). It is still debated what may be the most convenient parameter(s) to describe the light curve shape and discriminate between intrinsically brighter and fainter SNe and, more important, what is the correct absolute calibration.

Theoretical calculations have shown that the absolute magnitude at maximum is proportional to the amount of ^{56}Ni (Arnett 1982; Höflich et al. 1996; Cappellaro et al. 1997). However it is not yet clear how this relates with the progenitor scenarios and explosion mechanism. In particular, a growing number of "outliers" seems to indicate that a one-parameter description of SNe Ia is not sufficient to parameterize the light curve of SNe Ia (for an analysis of the type Ia luminosity dependence on second parameters see Parodi et al. 2000). In addition, recent observations show an increasing number of "disturbing" objects which merge properties of normal, sub-luminous and super-luminous SNe, like SN 2000cx or SN 2002cx. The first one is characterized by a slow decline but a relatively fast pre-maximum brightening, similar to that of the normal SN 1994D (Li et al. 2001). Nevertheless the absolute magnitude at maximum is consistent with a sub-luminous SN (Candia et al. 2002) and, in addition, the $B-V$ colour shows an unusual evolution, becoming at late time significantly bluer than the average of unreddened normal SNe Ia (Candia et al. 2002). The second one is characterized by a 1991T-like pre-maximum spectrum and a 1991bg-like luminosity, a normal $B-V$ colour evolution, very low expansion velocities and many other peculiarities (Li et al. 2003).

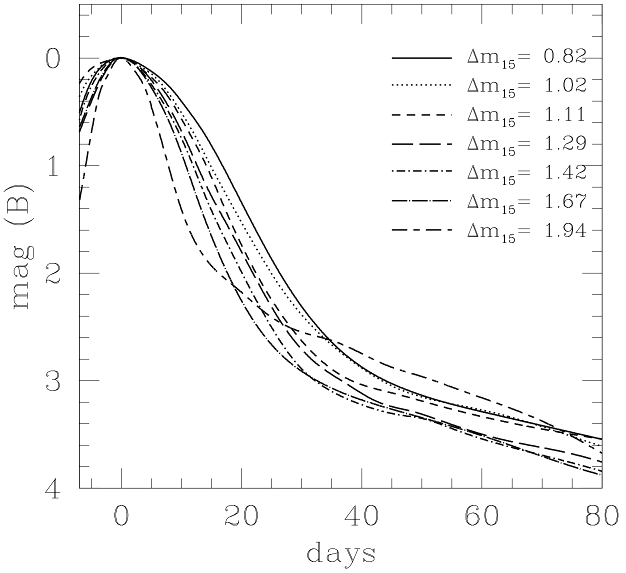

Figure 1. SN Ia template light curves in B band for seven different decline rates.

Therefore, even if we will exploit the fact that in general the light curve shape correlates with the absolute magnitude at maximum, it should be kept in mind that this is not a universal law. Not only it has an intrinsic dispersion but in addition there are really "anomalous" SNe.

2.1 Light curve shape

A few different approaches are currently in use to characterize the luminosity evolution of different SNe Ia. In principle the Multi-colour Light Curve Shape (MLCS) method of Riess et al. (1996a), which makes use of the entire early light curve (from discovery to 80-100 days) in different colours, is expected to be the most robust from a statistically point of view. This method has also the great advantage of giving at the same time the absolute calibration and the extinction. However the MLCS method heavily relies on the accurate calibration of a few template light curves, especially for what concerns the extinction correction, which explains the difference in the template colour curves in Riess et al. 1996a and Riess et al. 1998 (see also Salvo et al. 2001).

Two more straightforward measurements of the luminosity evolution are the Δm_{15} (the magnitude decline between the maximum and fifteen days later) (Phillips 1993),

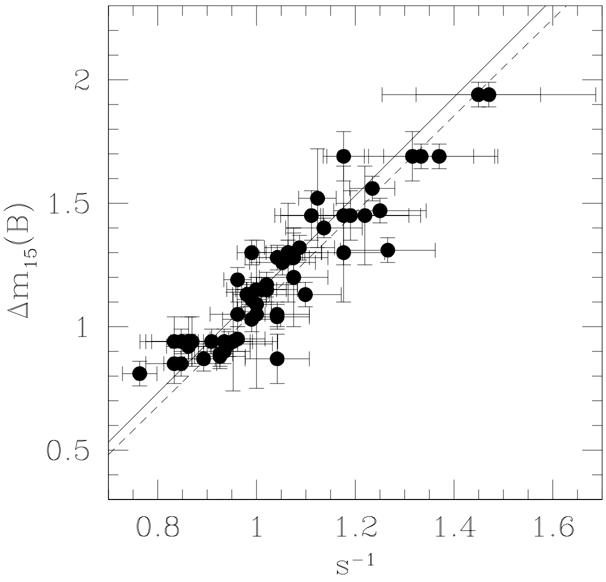

Figure 2. $\Delta m_{15}(B)$ versus *stretch factor s* for 58 SNe Ia. The inferred correlation (solid line) is in good agreement with that obtained by Perlmutter et al. (1997) (dashed line).

and the "stretch factor" s (Perlmutter et al. 1997), a coefficient used to expand or contract linearly the time-scale of a particular light curve in order to match a template[1]. In this work we choose to compare these last two methods.

To measure $\Delta m_{15}(B)$ and s for the SNe of our sample we proceeded as follows:

(i) B and V light curves of all SNe were corrected for the effect of red-shift on the time scale of evolution (time dilatation) and on the photometry (K-correction). For the latter we use the K corrections given by Hamuy et al. (1993);

(ii) among the SNe of our sample we selected 28 events for which the most complete temporal coverage was available. For each individual object we have measured the epoch and magnitude of maximum and the $\Delta m_{15}(B)$. The SN light curves were then grouped in seven bins of similar $\Delta m_{15}(B)$ (in order to have a good $\Delta m_{15}(B)$ sampling and enough statistics per bin). The individual observations were merged together to derive seven template light curves characterized by the average $\Delta m_{15}(B)$ (see Appendix C). Due to the paucity of light curves with coverage during the rise phase, the light curve trend before maximum is quite uncertain. The template light curves are shown in Fig. 1 where it can be seen that with the increasing of $\Delta m_{15}(B)$ the light curve shape varies with continuity. That is, the magnitude differences which originates from the different early decline rates are more or less maintained after the inflection point when the light curve turn on a more gentle decline. The exception are the SNe with the highest early decline ($\Delta m_{15}(B) = 1.94$) that, because of an earlier occurrence of the inflection point, 1-2 months after maximum appear brighter (relatively to maximum) than other SNe Ia.

(iii) for SNe with incomplete temporal coverage we have selected, by means of a χ^2 test, the best matching template and attributed to the object the corresponding $\Delta m_{15}(B)$. For practical reasons, the section of the light curve which goes from maximum to the inflection point is that for which detailed monitoring for the largest sample of events is available. Therefore, in the light curve fit, we gave more weight to the points in this phase range. Eventually, the shifts in phase and magnitude adopted to get the best match were used to refine the initial guess for the epoch and magnitude at maximum.

Instead, to measure the stretch factor s, we have adopted as reference the template light curve with $\Delta m_{15}(B) = 1.11$, i.e. our template closer to the "standard light curve", arbitrary chosen to be characterized by $\Delta m_{15}(B) = 1.1$ (Perlmutter et al. 1997). In practice, for each SN the time scale of the light curve was compressed by a factor s chosen to get the best χ^2 fit with the reference template light curve. Due to the uncertainties on the rising branch of the light curve templates and on the paucity of observations before maximum, the comparison has been performed mainly taking into account the light curve evolution from maximum to 80 days at most.

Following this procedure, we could measure both $\Delta m_{15}(B)$ and s for 58 SNe Ia (columns 3 and 4 in Table B1). Fig. 2 shows that $\Delta m_{15}(B)$ and s^{-1} are indeed well correlated. We notice that, as expected from Fig. 1, the stretched template light curve gives a very poor fit of the observed light curve for fast declining objects (like SN 1991bg), which can not be well fitted simultaneously in the early and late phases. This is the reason of the large error-bars for such objects. In any case, a least-squares fit considering the errors on both variables gives $\Delta m_{15}(B) = (1.98 \pm 0.16)(s^{-1} - 1) + (1.13 \pm 0.02)$ which is very close to the relation obtained by Perlmutter et al. (1997) ($\Delta m_{15}(B) = (1.96 \pm 0.17)(s^{-1} - 1) + 1.07$) from 18 low red-shift SNe.

We also note that the dispersion along the fitting line is consistent with the error estimates and, even in this enlarged sample, there are no obvious outliers. Hence, the systematic differences in the SN magnitudes calibrated using either Δm_{15} or the stretch factor (Drell, Loredo & Wasserman 2000; Leibundgut 2000) are not due to a misalignment of the different methods of measuring the light curve shapes and instead must originate in some other steps of the calibration chain. As we will see the reddening correction is a most critical issue.

Because of the good correlation between Δm_{15} and stretch factor and because Δm_{15} is available for a larger number of objects, for the SNe Ia calibration hereafter we will use the Δm_{15} light curve parameterization.

---

[1] Recently Wang et al. (2003) introduced a new method called the Colour-Magnitude Intercept Calibration (CMAGIC) which makes use of multi-colour post-maximum light curves. It is based on the empirical relation found between the B magnitude and the $B - V$ (or $B - R$ or $B - I$) colour during the first month past maximum. A complete analysis of this method, discussing also the B-R and B-I colours will be presented by the same authors in a later paper.

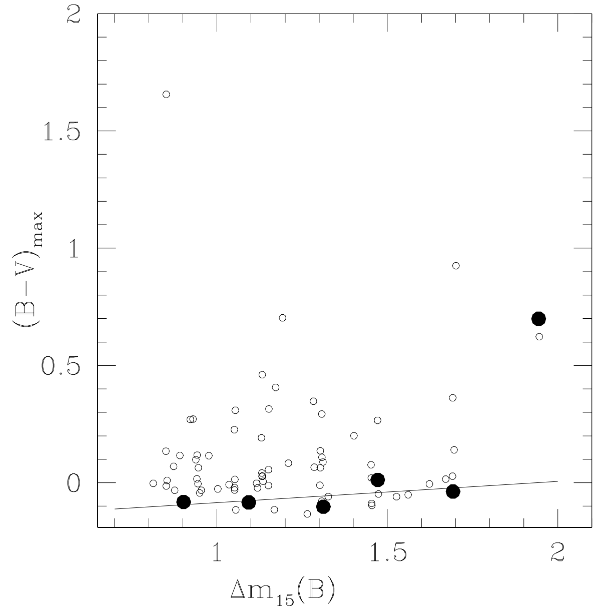

Figure 3. $(B-V)_{max}$ vs Δm_{15}. Correction for Galactic extinction has been applied. Black dots are SNe not affected by host galaxy reddening and spanning a wide range of decline rates. The solid line is the linear fit of these unreddened SNe (excluding the points with $\Delta m_{15} \sim 1.95$; see text). The scatter of the empty circles is due to the host galaxy reddening.

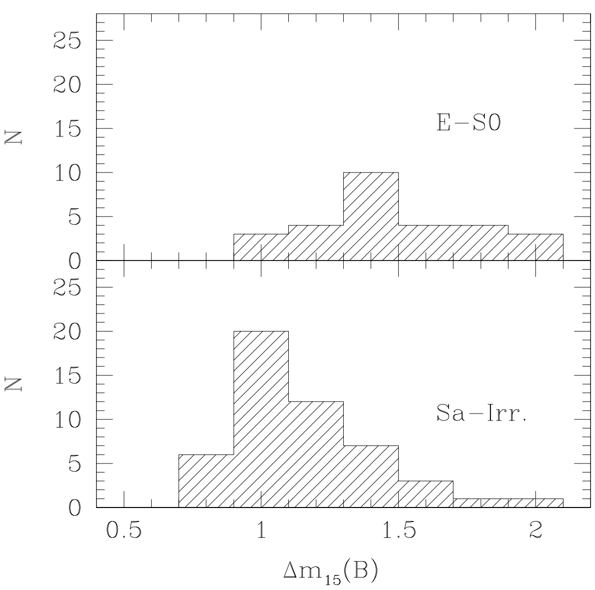

Figure 4. Histogram of $\Delta m_{15}(B)$ for SNe Ia in early type galaxies (upper panel) and in late galaxies (lower panel). The $\Delta m_{15}(B)$ values have been corrected for extinction, as explained in §2.2. A Kolmogorof–Smirnov test shows that the probability that the two distributions derive from the same population is very small ($P = 0.003\%$).

2.2 Reddening correction

The SN light is extinguished by the dust in our own Galaxy and in the host galaxy. For the Galactic extinction we have independent estimates either from HI maps and galaxy counts (Burstein & Heiles 1982) or from the COBE/DIRBE and IRAS/ISSA maps (Schlegel, Finkbeiner & Davis 1998). The latter has been adopted in the present work.

Instead, to estimate the extinction in the host galaxy, following the usual approach we make use of the observed SN colour. In practice, we derive two different estimates as follows:

(i) a plot of the $B-V$ colour at maximum (corrected for galactic extinction) versus the light curve decline rate $\Delta m_{15}(B)$ is shown in Fig. 3. The $B-V$ colour at maximum has been measured on the $B-V$ colour curve by a polynomial fit of the points around the maximum or by a template colour curve when the sampling was poor. We used different templates corresponding to SNe Ia with different Δm_{15}.

Most of the observed dispersion is due to host galaxy extinction, but there are also intrinsic differences. In particular it is now known that SN Ia with $\Delta m_{15}(B) > 1.8$ are intrinsically red at maximum, with $(B-V)_0 \simeq 0.7$. For all other SNe Ia and assuming that the lower rim of the distribution corresponds to SNe with negligible extinction, the differences in the intrinsic colours are certainly smaller but still there is an indication that in the intrinsic colour correlates with the luminosity decline rate: SNe with a faster decline rate are redder (Riess et al. 1998; Phillips et al. 1999; Nobili et al. 2003). This is shown in Fig. 3 by fitting the data of 5 SNe (SN 1999bc, 1992al, 1994D, 1992A, 1992bo) spanning a wide range of decline rates and for which there are indications that the host galaxy reddening was very low (Phillips et al. 1999). We found $(B-V)_{max} = 0.09(\pm 0.08) \times (\Delta m_{15} - 1.1) - 0.08(\pm 0.03)$ and this relation was adopted to derive the colour excess for all type Ia SNe but the very fast declining objects ($\Delta m_{15}(B) > 1.8$). For the latter we assumed that they have all the same intrinsic colour $(B-V)_0 = 0.70$. $E(B-V)_{max}$, corrected for the galactic component, are reported in column 6 of Table B1.

(ii) As shown by Lira (1995), the colour evolution of SN Ia between 30 and 90 days can be well approximated by the following linear relation: $(B-V)_0 = 0.725 - 0.0118 \times (t_V - 60)$, where t_V is the time (in days) from the V maximum. This is independent on the SN decline rates, including extreme objects like SN 1991bg. There is however at least one important exception, SN 2000cx (Candia et al. 2002) which should not be overlooked.

The shift of observed colour of SN Ia required to fit this relation gives an alternative estimate of the host galaxy extinction $E(B-V)_{tail}$ reported in column 7 of Table B1.

Finally, as estimate of the host galaxy extinction, $E(B-V)_{host}$, was adopted the weighted mean of $E(B-V)_{max}$ and $E(B-V)_{tail}$ (cf. Phillips et al. 1999). In the few cases, when the formal mean turns out to be negative, the $E(B-V)_{host}$ were set equal to zero. This is equivalent to adopt a Bayesian filter with a flat a priori distribution for positive $E(B-V)$ and zero for $E(B-V) < 0$. Our adopted $E(B-V)_{host}$ are reported in column 8 of Table B1.

Some authors applied a different Bayesian filter to the measured values of $E(B-V)$. In particular, Phillips et al. (1999) assumed a one-sided Gaussian "a priori distribution"

(Riess et al. 1996a). It turns out that their choice of a relatively small value of σ corresponds to an arbitrary reduction of $E(B-V)_{host}$, especially for objects with high colour excess. In turn, this results in smaller absorption corrections for the SN magnitudes. This choice, while not well justified, has the positive effect to reduce the dispersion of the corrected SN absolute magnitudes. We will come back to this point in the next section.

Phillips et al. (1999) have shown that, because of the rapid spectral evolution of SN Ia and of the (small) dependence of the reddening on the colour of the source the observed $\Delta m_{15}(B)$ must be corrected as follows: $\Delta m_{15}(B) \simeq \Delta m_{15}(B)_{obs} + 0.1 \times E(B-V)$. The $\Delta m_{15}(B)$ reported in column 4 of the Table B1 are the observed values.

A comparison of our estimates of $\Delta m_{15}(B)$ and colour excess with those reported by Phillips et al. (1999) for the objects in common shows that, except for a few cases, the values agree within the errors. The differences are due to slightly different choices for the epoch and magnitude at maximum.

2.3 Absolute magnitude vs. $\Delta m_{15}(B)$

In order to use SNe Ia as distance indicators, their absolute magnitude M_B needs to be calibrated. This requires that at least for a sub-sample of objects, the distance modulus of the host galaxies is measured by means of some independent distance indicators. As we will argue in the next section, this is best done with Cepheids.

If SNe Ia were true standard candles, the calibrated absolute magnitude could be directly used to measure the distance of all other SN host galaxies. As we mentioned before, this is not the case but, thanks to the relation between absolute magnitude at maximum and luminosity decline (Phillips 1993), the role of SNe Ia as distance indicators can be recovered. Therefore is this relation which needs to be calibrated.

Unfortunately this cannot be done using the Cepheid calibrated SNe Ia alone for two reasons:

(i) the number of SN Ia host galaxies with Cepheid measured distances is too small (only 9 objects, as shown in Table 2);

(ii) as shown in Fig. 4, SNe Ia with different absolute magnitudes are not uniformly distributed versus galaxy types. In particular faint, rapidly declining SNe Ia occur preferentially in early type galaxies (see also Filippenko 1989, Hamuy et al. 1996c, Cappellaro & Turatto 2001). As discussed by Ivanov, Hamuy & Pinto (2000) this effect may be due to the age of the progenitors (the older the progenitor system, the fainter the corresponding SN), but also to metallicity (lower metallicity systems produce fainter SNe, Umeda et al. 1999).

Since Cepheids are found in spirals only, it is not possible to properly sample the M_B – $\Delta m_{15}(B)$ relation by means of Cepheid calibrated SNe Ia.

To overcome these difficulties we adopted a two-step procedure. We first determine the slope of the relation using some widely available, though less accurate, distance indicators (Fig. 5); then, since the linear fit depends on the assumed value of H_0 (75 $\mathrm{km\,s^{-1}Mpc^{-1}}$), we determine the zero point by minimizing the deviation of the Cepheids calibrated SNe Ia on this fixed slope (see next section).

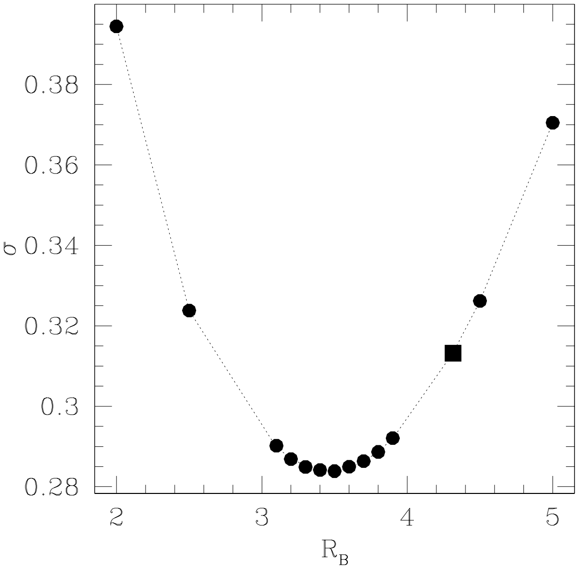

Figure 6. Dispersion of the M_B – Δm_{15} relation for different values of R_B. The sample is the same as in figure 5 **b**. The filled square corresponds to $R_B = 4.315$. The minimum corresponds to $R_B = 3.5$.

For the first step, absolute magnitudes have been calculated using distances obtained from two different sources. Distance moduli for 24 host galaxies were retrieved from the *"Nearby Galaxies Catalog"* (Tully 1988). For the galaxies not listed there and with recession velocity larger than 3000 $\mathrm{km\,s^{-1}}$ (49 objects), we have determined the distance from the recession velocity, adopting $H_0 = 75\ \mathrm{km\,s^{-1}Mpc^{-1}}$ to be consistent with the Tully's catalogue scale. In order to avoid contamination from peculiar motions, we rejected 5 of the 78 SNe of the sample which are not listed in Tully's catalogue and have low recession velocity. Recession velocities in the reference frame of the 3K background microwave radiation were retrieved from the NASA/IPAC Extragalactic Database[2].

To show the importance of the host galaxy extinction correction, in Fig. 5**a** we have plotted the data of 73 SNe, corrected for Galactic extinction only. As it can be seen, the the points show a large dispersion and the correlation between M_B and $\Delta m_{15}(B)$ remains hidden.

The scatter appears greatly reduced in Fig. 5**b** where the SN magnitudes have been corrected for extinction in the host galaxy. The latter has been derived from the colour excess estimated in §2.2 and assuming a standard reddening law, that is $A_B = 4.315 \times E(B-V)$ (Schlegel et al. 1998, see also Cardelli, Clayton & Mathis 1989). The only evident outliers are now four fast declining SNe (the sub-luminous SNe 1992K, 1999da, 1998de, 1991bg), SN 1996ai, whose colour excess is very high but not well defined (Phillips et al. 1999), and 1986G, another highly reddened SN.

Actually, we found that the dispersion in the M_B – $\Delta m_{15}(B)$ relation can be further reduced assuming a different value for R_B. As shown in Fig. 6, a minimum dispersion

---

[2] http://nedwww.ipac.caltech.edu/

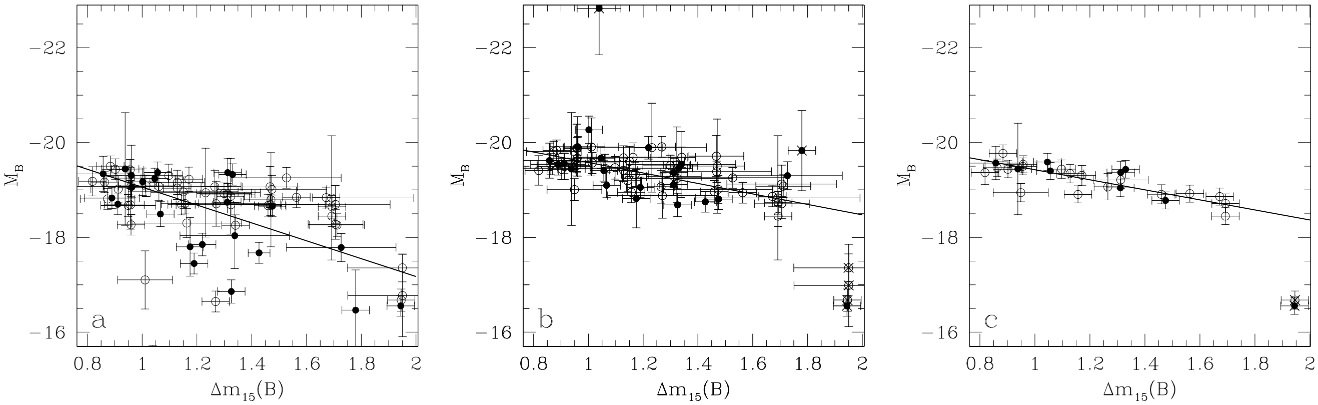

Figure 5. M_B versus $\Delta m_{15}(B)$ relation; filled circles indicate objects whose distances are given by Tully's catalogue, open symbols are objects whose distances are calculated from their recession velocity. The linear fit is weighted in both axes (Press 1992). **a**: Only galactic reddening correction applied. Number of objects used for the linear fit n=73, dispersion $\sigma = 0.83$. **b**: Both Galactic and host galaxy reddening corrections applied. The outliers, marked with a cross, are (from left to right, from top to bottom): SN 1996ai, which is characterized by high and not well known reddening; SN 1986G, another highly reddened event; SN 1992K, 1999da, 1998de, 1991bg, which are peculiar sub-luminous events. The latters seem to form a separate class and do not fit the linear relation defined by all others. n=67, $\sigma = 0.31$. **c**: as the previous case but selecting only SNe with $E(B-V) < 0.1$ and small errors (< 0.2) in $\Delta m_{15}(B)$. n=26, $\sigma = 0.20$, $R_B = 3.5$.

Table 1. Parameters of the M_B=a$(\Delta m_{15}(B) - 1.1) + b$ relation. From top to bottom: values obtained for case **b**, **c** (as in §2.3). From left to right: number of objects used for the correlation; R_B adopted; slope (error); zero point derived from three different assumptions on the metallicity PL relation (error); dispersion.

n	R_B	a	b				σ
			KP	$\Delta Y/\Delta Z = 2.5$	$\Delta Y/\Delta Z = 3.5$		
67	4.315	1.102 (0.147)	-19.613	-19.523	-19.582	(0.037)	0.31
67	3.5	1.092 (0.124)	-19.460	-19.399	-19.472	(0.031)	0.28
26	3.5	1.061 (0.154)	-19.455	-19.403	-19.476	(0.044)	0.20

is obtained for $R_B = 3.5$, somewhat smaller than the canonical values $R_B = 4.315$.

A qualitatively similar result was obtained, again using SN Ia, by Capaccioli et al. (1990), who favoured $R_B = 1.7$. However, previous measurements of low values for R_B from SNe were plagued by an inadequate understanding of the relation between intrinsic color and luminosity at maximum (Riess et al. 1996b). Other measurements of absorption in nearby galaxies provided values for R_B ranging from the canonical value ($R_B \sim 4.3$) to much smaller values ($R_B \sim 3.6$: Bouchet et al. 1985, Brosch, N. 1988, Brosch, N. & Loinger, F. 1991; $R_B \sim 2.4$: Rifatto 1990). However a lower estimate for the host galaxy reddening correction R_B has been suggested also by more recent studies ($R_B \sim 3.5$ Phillips et al. 1999; Knop et al. 2003).

Actually, even in our own Galaxy the ratio of the total to selective absorption has been found to vary significantly from place to place (e.g. R_V varies from 2.6 to 5.5 in the measurements of Clayton & Cardelli 1988). Therefore, in principle, it would be interesting to study the dependence of R_B on other observables, such as the distance from the host galaxy centre or the integrated galaxy properties. This would require the possibility to derive estimate of R_B for individual objects which, unfortunately, cannot be done with the present data.

We note that, from a practical point of view, reducing R_B has the same effect of the adoption of a relatively narrow a-priori distribution of the reddening for a Bayesan estimate of the individual SN extinction (cf. §2.2). In §3 we will check what is the effect on the Hubble diagram of this different choice for R_B.

The issue is important (see also Fischer 2003) because it turns out that, on average, the more distant SNe of our sample are less affected by the extinction than nearby ones. This is shown in Fig. 7: it turns out that for SNe in galaxies with recession velocity smaller than 3000 $km\,s^{-1}$ the average colour excess is ~ 0.27, whereas the same number for more distant galaxies is ~ 0.13.

This is likely due to selection effects, since distant obscured objects are more difficult to detect and SNe are likely to be discovered far from their host nucleus in distant galaxies.

As a final test we plot the $M_B - \Delta m_{15}(B)$ for the subsample of 26 SNe with $E(B-V) < 0.1$ and well measured Δm_{15} (Δm_{15} uncertainties < 0.2) (see also Phillips et al. 1999, Freedman et al. 2001). This has two advantages, it gives a more homogeneous sample and the uncertainties related to the host galaxy extinction correction are reduced. The result, shown in Fig.5**c**, is a very tight relation with dispersion $\sigma = 0.20$.

Table 2. Cepheid calibrated SNe. (1) SN name; (2) host galaxy; (3) apparent B magnitude at maximum; (4) $B-V$ colour at maximum; (5) $\Delta m_{15}(B)_{obs}$ (not corrected for colour excess); (6) $E(B-V)_{gal}$ from Schlegel et al. 1998; (7) $E(B-V)_{host}$: weighted mean between $E(B-V)_{max}$ and $E(B-V)_{tail}$; (8) μ_0(KP), (9) $\mu_0(\Delta Y/\Delta Z)=2.5$, (10) $\mu_0(\Delta Y/\Delta Z)=3.5$ are the distance moduli given by the HST Key Project (Freedman et al. 2001) and the distance moduli obtained for two different metallicity (see §2.4).

SN (1)	galaxy (2)	m(B)$_{max}$ (3)	$B-V$ (4)	$\Delta m_{15}(B)_{obs}$ (5)	$E(B-V)_{gal}$ (6)	$E(B-V)_{host}$ (7)	μ_0(KP) (8)	$\mu_0(\frac{\Delta Y}{\Delta Z}=2.5)$ (9)	$\mu_0(\frac{\Delta Y}{\Delta Z}=3.5)$ (10)
1990N	NGC4639	12.75(0.04)	0.04(0.05)	1.05(0.05)	0.026(0.003)	0.14(0.06)	31.61(0.08)	31.47(0.26)	31.55(0.31)
1981B	NGC4536	12.04(0.04)	0.06(0.05)	1.13(0.05)	0.018(0.002)	0.11(0.05)	30.80(0.04)	30.66(0.20)	30.71(0.23)
1989B	NGC3627	12.38(0.12)	0.38(0.05)	1.28(0.05)	0.032(0.003)	0.42(0.05)	29.86(0.08)	29.88(0.42)	30.11(0.54)
1998bu	NGC3368	12.20(0.04)	0.34(0.05)	1.15(0.05)	0.025(0.003)	0.37(0.05)	29.97(0.06)	29.94(0.50)	30.12(0.63)
1972E	NGC5253	8.40(0.04)	-0.06(0.10)	1.05(0.05)	0.056(0.006)	0.01(0.05)	27.56(0.14)	27.65(0.15)	27.65(0.14)
1937C	IC4182	8.94(0.30)	0.00(0.20)	0.85(0.20)	0.014(0.001)	0.06(0.05)	28.28(0.06)	28.31(0.08)	28.31(0.08)
1960F	NGC4496	11.65(0.20)	...	1.10(0.20)	0.025(0.005)	...	30.81(0.03)	30.70(0.18)	30.72(0.20)
1974G	NGC4414	12.34(0.04)	0.22(0.20)	1.40(0.04)	0.019(0.005)	0.25(0.05)	31.10(0.05)	31.07(0.38)	31.25(0.48)
1991T	NGC4527	11.69(0.04)	0.14(0.05)	0.94(0.05)	0.022(0.002)	0.20(0.05)	30.74(0.12)	30.60(0.57)	30.65(0.66)

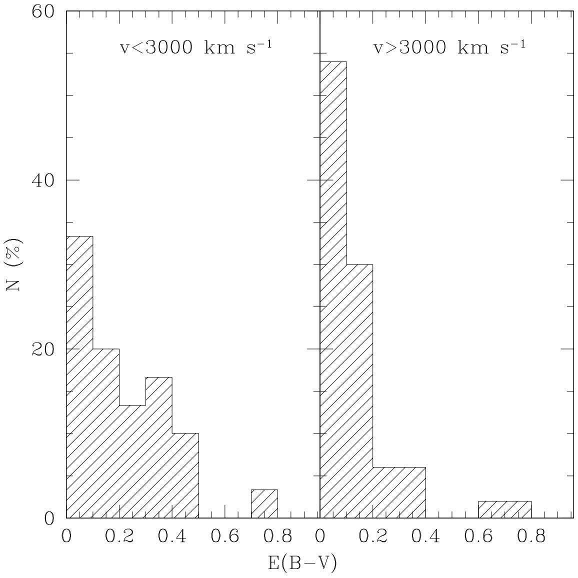

Figure 7. Distribution of the host galaxy extinction $E(B-V)_{host}$. Left: SNe with recession velocity smaller than 3000 km s^{-1}; Right: SNe with recession velocity bigger than 3000 km s^{-1}.

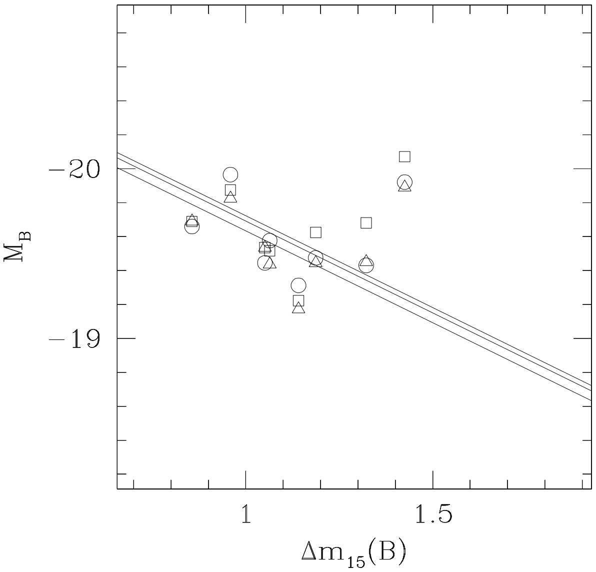

Figure 8. M_B versus $\Delta m_{15}(B)$ for 8 of the 9 SNe calibrated by Cepheids (SN 1960F has been excluded because colour information required to estimate the host galaxy extinction is not available). Circles: Distance modulus μ from Freedman et al. 2001; triangles: μ corrected assuming $\Delta Y/\Delta Z=2.5$; square: μ corrected assuming $\Delta Y/\Delta Z=3.5$. Solid lines are the best fits obtained with a fixed slope minimizing the deviation of the three sets of Cepheids calibrated SNe. The slope (1.082) is the same as in Fig. 5**c**.

The comparison of our results, reported in Table 1, with those obtained from 26 SNe of the Calán/Tololo survey (Hamuy et al. 1996c), indicates that we find a slightly steeper slope, in the range 1.061 ± 0.154 to 1.102 ± 0.147 depending on the sample vs 0.784 ± 0.182 of Hamuy et al. (1996c). It is interesting to note that the difference disappear if, as in Hamuy et al. (1996c), we neglect the host galaxy extinction correction ($a = 0.855 \pm 0.182$).

The next step is determine the zero point of the $M_B - \Delta m_{15}(B)$ relation by means of Cepheids calibrated SNe.

2.4 Effect of the metal content on the Cepheids-distance scale

Classical Cepheids are fundamental primary distance indicators thanks to their characteristic Period-Luminosity (PL) and Period-Luminosity-Colour (PLC) relations. Such relations, once calibrated, allow one to evaluate distances of the order of 3 Mpc from ground-based observations and about 30 Mpc from space observations (HST, Freedman et al. 2001 and references therein). Moreover, the Cepheid distance scale constrains the evaluation of the Hubble constant H_0 through the calibration of secondary distance indicators. This implies that any systematic error on the Cepheids as standard candles may affect the inferred extragalactic distance scale and, in turn, the value of H_0.

In the recent years, one of the most debated issues concerning the extragalactic distance scale is the possible dependence of Cepheid properties on the chemical composition of the host stellar population. Indeed, Cepheid PL relations are traditionally considered to be "universal" (Iben & Renzini 1984; Freedman & Madore 1990), with the slope derived from Cepheids in the Large Magellanic Cloud (LMC), (Madore & Freedman 1991; Udalski 2000) and the zero point corresponding to some assumption on the LMC distance modulus or on Galactic Cepheids with independent distance estimates. Empirical tests of the metallicity effect on the Cepheid distance scale suggest that either the effect is very small (Freedman & Madore 1990) or it goes in the direction of predicting brighter Cepheids for higher metallicities (Kennicutt et al. 1998).

On the basis of the latter test, the HST Key Project (KP) distance moduli are corrected for the metallicity effect by adopting the correction $\Delta\mu_0/\Delta[O/H] = 0.2 \pm 0.2$ (Freedman et al. 2001).

From the theoretical point of view, nonlinear convective pulsation models (Bono, Marconi & Stellingwerf 1999a), which are able to predict all the relevant pulsation observables, suggest that in the range $0.004 < Z < 0.02$ metal poor Cepheids are brighter than the metal-rich ones at fixed pulsation period (Bono et al. 1999b; Caputo, Marconi & Musella 2000a). As a consequence, at least in this range of Z, the adoption of "universal" LMC-based PL relations provides distances that are systematically overestimated (underestimated) for galaxies more metal-rich (metal-poor) than the LMC (Caputo et al. 2000b). On the other hand, when the pulsation analysis is extended to metallicities higher than the solar value (up to Z=0.04) in order to cover the whole range of metal abundances of the HST Key Project galaxies (Ferrarese et al. 2000), and the simultaneous effect of the increase in the helium abundance is taken into account, the predicted metallicity correction changes sign around the solar value and depends significantly on the adopted helium to metallicity enrichment ratio $\Delta Y/\Delta Z$ (see Fiorentino et al. 2002 for details). In particular Fiorentino et al. (2002) find that for $\Delta Y/\Delta Z$=3.5, the theoretical metallicity correction is in agreement with the result of the empirical test by Kennicutt et al. (1998).

In order to calibrate the M_B-$\Delta m_{15}(B)$ relation, we have considered three different estimates for the Cepheid distance to the SN host galaxies: μ_0(KP), computed without metallicity correction, and $\mu_0(\Delta Y/\Delta Z = 2.5)$, $\mu_0(\Delta Y/\Delta Z = 3.5)$ with the metallicity corrections for two different choices of the adopted helium to metallicity enrichment ratio $\Delta Y/\Delta Z$ (Table 2). The zero point of the $M_B - \Delta m_{15}(B)$ relation was determined by minimizing the deviation of the linear fit for the Cepheids calibrated SN, maintaining a fixed slope (Fig. 8). The inferred parameters of the correlation are reported in Table 1. The zero point obtained with different assumptions in the calibration lies in the range $-19.613 < b < -19.399$, to be compared with $b = -19.258 \pm 0.048$ in Hamuy et al. 1996c.

3 THE HUBBLE CONSTANT

After completion of the calibration path, we can now use SNe Ia to measure the Hubble constant.

In Fig. 9 we show three examples aimed to show how different corrections and sample selection affect the scatter of the Hubble diagram. For this purpose, we adopted the PL relation corrected for $\Delta Y/\Delta Z$=2.5 (see Table 1) and we excluded from the fit all SNe Ia with recession velocity $v <$ 3000 km s^{-1}. The latter is intended to avoid contamination by peculiar motions, which, on average, amount to ∼200–300 km s^{-1} (Tonry et al. 2000, Giovanelli et al. 1999). We have also excluded SNe with $\Delta m_{15}(B) > 1.8$ because they do not fit the linear relation $M_B - \Delta m_{15}(B)$, as seen in Fig. 5**b**.

In panel *a* of Fig. 9 is the Hubble diagram obtained using the complete sample and a standard reddening law, in panel *b* is the plot obtained adopting $R_B = 3.5$ for the ratio of total to selective extinction (cfr. §2.3) and finally, in panel *c* is shown the Hubble diagram for the sample of SN Ia with the best photometric coverage $\Delta m_{15}(B) < 0.2$ and low reddening $E(B-V)_{host} > 0.1$ ($R_B = 3.5$).

The fact that the dispersion of the points in panel *b* ($\sigma = 0.24$) is significantly reduced compared with panel *a* ($\sigma = 0.29$) is consistent with the finding of §2.3. Again, it appears that the host galaxy absorption correction deduced from the measured colour excess and adopting a standard reddening law is an overestimate of the true absorption. On the other side, this turns out to have a small effect on the value of the Hubble constant itself ($H_0 = 74^{+9}_{-8}$ in panel *b* compared with $H_0 = 74^{+11}_{-9}$ in panel *a*) provided that in all steps the calibration of the SN magnitudes is done consistently (see also Table 3).

The dispersion of the Hubble diagram is further reduced by selecting the subsample of SN Ia with good photometry and low reddening SNe ($\sigma = 0.20$). This time the Hubble constant is slightly reduced $H_0 = 71^{+7}_{-6}$. Although this is our preferred result and that with the smallest statistical uncertainty, we stress that the selection criteria were not applied to the Cepheid calibrated SN of Table 2 which otherwise would be reduced to only two cases. In principle, this asymmetry may introduce some bias.

The different results are summarized in Table 3 where in particular it can be seen the sensitivity of the estimate of the Hubble constant on the different corrections of the PL relation. As it can be seen the effect is, in all cases, quite small.

H_0 ranges between 68 and 74 km s^{-1} Mpc^{-1}, with uncertainties of the order of ~ 7 km s^{-1} Mpc^{-1} ($\sim 10\%$)[3]

These values are in agreement with the result of the Hubble Space Telescope Key Project (Freedman et al. 2001) which gives $H_0 = 72 \pm 8$ km s^{-1} Mpc^{-1}. They are also in agreement with the recent results of *WMAP*, namely $H_0 = 72 \pm 5$ km s^{-1} Mpc^{-1} (Spergel et al. 2003), obtained for a spatially flat cosmological model dominated by cold dark matter and non-zero cosmological constant (ΛCDM model).

---

[3] The fact that the distance scale turned out to be very close to that of the Nearby Galaxies Catalogue by Tully (1988) which was used to derive the slope of the M_B-$\Delta m_{15}(B)$ relation assure on the negligible impact of possible second order effects.

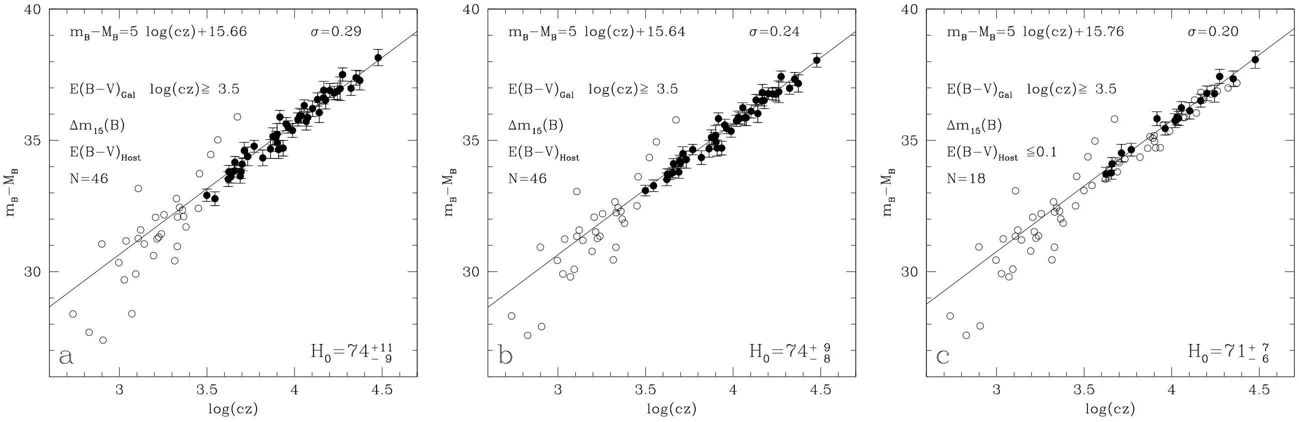

Figure 9. **a**: Hubble diagram of the whole sample assuming $R_B = 4.315$ in the estimate of the host galaxy absorption. **b**: as the previous plot but with $R_B = 3.5$. **c**: Hubble diagram for the good photometry, low extinction sample ($R_B = 3.5$). In all plots, we have used for the fit only those SN with recession velocity > 3000 km s^{-1} and we have adopted the Cepheids P-L correction for $\Delta Y/\Delta Z$=2.5. The fast declining SNe 1991bg, 1992K, 1999da and 1998de have been excluded from the fit. Points which do not contribute to the fit are indicated as open circles.

Note that the same *WMAP* data give smaller value for H_0 if fitted by different cosmological models.

4 CONCLUSIONS

Using a large sample of SNe Ia light curves, both from the literature or unpublished data, we have revisited the different steps required to calibrate the SN absolute magnitude and derive the Hubble constant.

In particular, we have re-calibrated the relation between the SN absolute magnitudes and their rate of decline soon after maximum. The latter can be measured without distinction by the $\Delta m_{15}(B)$ or by the “stretch factor”

SN Ia with Cepheids calibrated distances are crucial because they are used to calibrate the zero point of the M_B vs. $\Delta m_{15}(B)$ relation. We have considered the effect of a new metallicity correction of the Cepheids PL relation, how this reflects on the calibration of SN Ia and finally on the estimate of the Hubble constant. Fortunately, the latter turned out to be not very important.

Instead we found that a major uncertainty is related to the correction of the extinction in the host galaxy. In particular, we found that the scatter of the M_B – Δm_{15} relation and of the Hubble diagram itself can be reduced assuming a (slightly) smaller value for the ratio of the total to selective absorption, R_B. Indeed, the scatter is minimum for $R_B = 3.5$. The difference with the standard value, $R_B = 4.315$, is well within the variance of the measurements of this parameter even within our own Galaxy. Therefore it does not require different properties for the dust in other galaxies. Still this is an important issue for the use of SN as distance indicators.

The Hubble constant, obtained with different assumptions on the metallicity dependence of the Cepheid PL relation, different cuts in the sample and varying the value of R_B, lies in the range 68–74 km s^{-1}Mpc^{-1}, with uncertainties of the order of 10%.

Table 3. Values of H_0 (in km s^{-1} Mpc^{-1}) for different assumptions on the Cepheid calibration and R_B. *a* and *b* are the values for the complete sample, whereas in *c* are the values for the good photometry, low reddening sample.

	a	**b**	**c**
N(SN)	46	46	18
R_B	4.315	3.5	3.5
μ_0(KP)	71^{+10}_{-9}	72^{+8}_{-7}	69^{+7}_{-6}
$\mu_0(\frac{\Delta Y}{\Delta Z} = 2.5)$	74^{+11}_{-9}	74^{+9}_{-8}	71^{+7}_{-6}
$\mu_0(\frac{\Delta Y}{\Delta Z} = 3.5)$	72^{+10}_{-9}	72^{+8}_{-7}	68^{+6}_{-6}

5 ACKNOWLEDGMENTS

Unpublished data are based on observations collected at ESO - La Silla (Chile), Asiago (Italy), TNG (La Palma, Canary Islands, Spain) and HST WFPC2 Archive. We acknowledge support from the Italian Ministry For Instruction, University and Research (MIUR) through grant Cofin 2001021149-002 and from the European Research Training Network “The Physics of Type Ia Supernova” through grant RTN 2-2001-00037. This research has made use of the NASA/IPAC Extragalactic Database (NED) which is operated by the Jet Propulsion Laboratory, California Institute of Technology, under contract with the National Aeronautics and Space Administration.

References

Arnett W.D., 1982, ApJ, 253, 785
Barbon, R., Ciatti, F., Rosino, L., 1973, A&A, 29, 57
Bono, G., Marconi, M., Stellingwerf, R.F., 1999a, ApJS, 122, 167
Bono, G., Caputo, F., Castellani, V., Marconi, M., 1999b, ApJ, 512, 711

Bouchet, P., Lequeux, J., Maurice, E., Prevot, L., Prevot-Burnichon, M. L., 1985, A&A, 149, 330

Brosch, N., in Dust in the Universe, ed. M. E. Bailey & D.A. Williams (Cambridge: Cambridge Univ. Press), 502

Brosch, N. & Loinger, F., 1991, A&A, 249, 327

Burstein, D., Heiles, C., 1982, AJ, 87, 1165

Candia P. et al., astro-ph/0212543

Capaccioli, M., Cappellaro, E., della Valle, M., D'Onofrio, M., Rosino, L., Turatto, M., 1990, ApJ, 350, 110

Cappellaro, E., Mazzali, P. A., Benetti, S., Danziger, I. J., Turatto, M., Della Valle, M., Patat, F., 1997, A&A, 328, 203

Cappellaro, E., Turatto, M., 2001, The effect of binaries on stellar population studies, editor D. Vanbeveren, ASSL series vol. 264, Kluwer Academic Publishers: Dordrecht, p. 199.

Caputo, F., Marconi, M., Musella, I. 2000a, A&A, 354, 610

Caputo, F., Marconi, M., Musella, I., Santolamazza, P., 2000b, A&A, 359, 1059

Cardelli, J.A., Clayton, G.C., Mathis, J.S., 1989, ApJ, 345, 245

Clayton, G.C.,Cardelli, J.A., 1988, AJ, 96, 695

Drell, P.S., Loredo, T.J., Wasserman, I., 2000, ApJ, 530, 593

Ferrarese, L. et al., 2000, ApJS, 128, 431

Filippenko, A. V., 1989, PASP, 101, 588

Fiorentino, G., Caputo, F., Marconi, M., Musella, I., 2002, ApJ, 576, 402

Fischer E., astro-ph/0306459

Freedman, W. L., Madore, B. F., 1990, ApJ, 365, 186

Freedman et al., 2001, ApJ, 553, 47

Giovanelli, R., Dale, D.A., Haynes, M.P., Hardy, E, Campusano, L.E., 1999, ApJ, 525, 25

Hamuy, M., Phillips, M.M., Wells, L.A., Maza, J., 1993, PASP, 105, 787

Hamuy, M., Phillips, M.M., Suntzeff, N.B., Schommer, R.A., Maza, J., Aviles, R., 1996a, AJ, 112, 2398

Hamuy M. et al., 1996b, AJ, 112, 2408

Hamuy M., Phillips, M.M., Suntzeff, N.B.,Schommer, R.A., Maza, J., Aviles, R., 1996c, AJ, 112, 2391

Höflich, P., Khokhlov, A., Wheeler, J. C., Phillips, M.M., Suntzeff, N.B., Hamuy, M., 1996, ApJ, 472, L81

Iben, I., Renzini, A., 1984, Physics Reports, 105, 329

Ivanov, V.D., Hamuy, M., Pinto, P.A., 2000, ApJ 542, 588

Kennicutt, R. C. et al., 1998, ApJ, 498, 181

Knop R.A. et al., 2003, ApJ, 598, 102

Landolt, A. U., 1992, AJ, 104, 340

Leibundgut, B., 2000, A&AAR, 10, 179

Li W. et al., PASP 113, 1178

Li W. et al., PASP 115, 453

Lira, P., 1995, Masters thesis, Univ. Chile

Madore, B. F., Freedman, W. L., 1991, PASP, 103, 933

Nobili S., Goobar A., Knop R., Nugent P., 2003, A&A, 404, 901

Parodi, B.R., Saha, A., Sandage, A., Tammann, G.A., 2000, ApJ, 540, 634

Perlmutter, S. et al., 1997, ApJ, 483, 565

Perlmutter, S. et al., 1999, ApJ, 517, 565

Phillips M. M., 1993, ApJ, 413, L105

Phillips, M.M., Lira, P., Suntzeff, N.B., Schommer, R.A., Hamuy, M., Maza, J., 1999, AJ, 118, 1766

Press, W.H., Teukolsky S.A., Vetterling W.T., Flannery, B.P., 1992, Numerical Recipes in Fortran 77, The Art of Scientific Computing, 2nd Ed., Cambridge University Press

Pskovskii, I.P., 1977, AZh, 54, 1188

Riess, Adam G., Press, William H., Kirshner, Robert P., 1996a, ApJ, 473, 88

Riess, Adam G., Press, William H., Kirshner, Robert P., 1996b, ApJ, 473, 588

Riess, A.G., Davis, M., Baker, J., Kirshner, R.P., 1997, ApJ, 488, L1

Riess, A.G. et al., 1998, AJ, 116, 1009

Riess A. G. et al., 1999, AJ, 117, 707

Rifatto, A., 1990, in Dusty Objects in The Universe, ed. E. Bussoletti & A.A. Vittone (Netherlands: Kluwer), 277

Rust, B.W., 1974, Ph.D. Thesis,

Salvo, M.E., Cappellaro, E., Mazzali, P.A., Benetti, S., Danziger, I.J., Patat, F., Turatto, M., 2001, MNRAS, 321, 254

Sandage, A., Tammann, G.A., 1993, ApJ, 415, 1

Schlegel, D.J., Finkbeiner, D.P., Davis, M., 1998, ApJ, 500, 525

Schmidt, B.P. et al., 1998, ApJ, 507, 46

Spergel D.N. et al., astro-ph/0305097

Tonry, J.L., Blakeslee, J.P., Ajhar, E. A., Dressler A., 2000, ApJ, 530, 625

Tripp, R., Branch, D., 1999, ApJ, 525, 209

Tully, R.B, 1988, Nearby Galaxies Catalogue, Cambridge University Press

Turatto, M., Cappellaro, E., Benetti, S., Danziger, I. J., 1993, MNRAS, 265, 471

Turatto M., 2000, MmSAI, 71, 573

Udalski, A., 2000, AcA, 50, 279

Umeda, H., Nomoto, K., Kobayashi, C., Hachisu, I., Kato, M., 1999, ApJ 522, 43

Wang, L., Goldhaber, G., Aldering, G., Perlmutter, S., astro-ph/0302341

APPENDIX A: ESO - ASIAGO PHOTOMETRIC DATA

Table A1 reports the unpublished photometry based on observations collected mainly at ESO - La Silla (Chile) and Asiago (Italy), plus some data from TNG (La Palma, Canary Islands, Spain) and from the HST WFPC2 Archive.

Data reduction has been performed using IRAF[4] standard recipes for trimming, bias and overscan correction and flat fielding. SN magnitudes have been measured mainly using a Point Spread Function (PSF) fitting technique, which ensures a good removal of bad pixels and cosmic rays (Turatto et al. 1993).

Photometric calibration was obtained from observation of Landolt standard stars (Landolt 1992) in photometric nights. This was also used to establish a local sequence which was used to calibrate the other observations.

In brackets are indicative estimates of the errors, obtained from the values measured on several reference nights through artificial stars experiments, i.e. adding a fake star, as bright as the SN, in several different positions around the SN location, and measuring the spread of the resulting magnitudes with the same procedure used for the SN.

The codes for the telescope/instrument used are as follows:

1= Danish 1.54m + DFOSC, 2= MPG/ESO 2.2m + EFOSC2, 3= ESO 3.6m + EFOSC1, 4= NTT + SUSI, 5= Dutch 0.91m, 6= NTT + EMMI, 7= Asiago 1.82m + AFOSC, 8= ESO 3.6m + EFOSC2, 9= TNG + OIG, 10= ESO 1.0m, 11= HST WFPC2 Archive.

Table A1.

Date	Julian Day +2,400,000	*U*	*B*	*V*	*R*	*I*	telescope
				SN 1991S			
13/04/91	48359.67	-	-	18.15(0.03)	-	-	1
18/04/91	48364.51	-	18.94(0.02)	18.42(0.03)	18.31(0.02)	-	2
20/04/91	48366.64	-	19.34(0.03)	18.51(0.02)	18.25(0.03)	-	3
				SN 1991T continues			
16/04/91	48362.85	12.26(0.02)	12.98(0.02)	12.84(0.02)	12.67(0.02)	12.87(0.02)	10
17/04/91	48363.80	12.04(0.02)	12.80(0.02)	12.74(0.02)	-	-	10
17/04/91	48363.65	-	12.73(0.01)	12.61(0.01)	-	-	2
18/04/91	48364.64	-	12.46(0.01)	12.34(0.01)	12.32(0.01)	-	2
20/04/91	48366.67	-	12.06(0.01)	12.00(0.01)	11.97(0.01)	-	3
21/04/91	48367.65	-	-	11.89(0.01)	-	-	3
22/04/91	48368.70	-	11.78(0.01)	11.80(0.01)	11.70(0.01)	-	3
20/05/91	48396.56	-	13.39(0.01)	12.32(0.01)	12.32(0.01)	-	3
20/05/91	48396.56	-	13.48(0.01)	12.29(0.01)	-	-	3
20/05/91	48396.56	-	-	12.45(0.01)	-	-	3
20/06/91	48427.67	-	14.77(0.01)	13.60(0.01)	13.51(0.01)	-	3
20/06/91	48427.67	-	-	13.66(0.01)	13.45(0.01)	-	3
20/06/91	48427.67	-	-	13.59(0.01)	-	-	3
01/08/91	48469.51	-	15.42(0.02)	-	14.78(0.02)	-	2
12/08/91	48480.49	-	-	15.29(0.02)	-	-	2
02/12/91	48593.46	-	16.98(0.06)	17.01(0.05)	17.62(0.06)	-	7
02/12/91	48593.46	-	16.95(0.06)	17.01(0.05)	17.59(0.06)	-	7
03/12/91	48594.46	-	17.06(0.06)	17.10(0.06)	17.65(0.06)	-	7
12/12/91	48603.46	-	17.04(0.06)	17.07(0.06)	17.68(0.06)	-	7

---

[4] Image Reduction and Analysis Facility, http://iraf.noao.edu/

Table A1.

Date	Julian Day +2,400,000	U	B	V	R	I	telescope
SN 1991T							
01/02/92	48653.90	-	17.66(0.05)	17.95(0.05)	18.54(0.05)	-	2
05/02/92	48657.82	-	17.74(0.04)	17.96(0.03)	18.56(0.04)	-	3
05/02/92	48657.60	-	-	17.88(0.07)	-	-	7
06/02/92	48658.66	-	17.75(0.07)	17.94(0.08)	18.52(0.06)	-	7
29/02/92	48681.78	-	18.02(0.06)	18.34(0.05)	18.97(0.05)	-	2
04/03/92	48686.46	-	18.25(0.10)	18.27(0.06)	19.00(0.08)	-	7
06/03/92	48688.46	-	18.25(0.10)	18.35(0.06)	19.05(0.08)	-	7
11/03/92	48692.67	-	18.42(0.07)	18.42(0.07)	19.07(0.06)	-	6
04/05/92	48746.69	-	18.99(0.05)	19.12(0.05)	19.58(0.05)	19.00(0.08)	3
26/07/92	48829.67	-	19.97(0.10)	20.27(0.05)	20.57(0.05)	-	2
23/12/92	48979.67	-	21.04(0.10)	20.95(0.08)	-	-	3
22/01/93	49010.67	-	21.02(0.10)	21.00(0.08)	21.28(0.09)	-	3
17/02/93	49035.67	-	-	20.97(0.09)	21.25(0.07)	-	6
27/02/93	49045.79	-	21.08(0.10)	20.99(0.09)	-	-	2
28/02/93	49046.79	-	21.21(0.10)	21.02(0.10)	21.36(0.10)	-	2
15/03/93	49061.67	-	21.03(0.10)	21.08(0.07)	21.17(0.07)	-	3
26/04/93	49103.60	-	21.06(0.10)	-	21.22(0.07)	-	3
27/04/93	49104.60	-	21.06(0.10)	21.21(0.08)	-	-	3
17/03/94	49428.78	-	21.43(0.11)	21.45(0.10)	-	-	6
10/05/94	49482.62	-	21.13(0.11)	-	-	-	3
15/05/94	49487.65	-	21.30(0.11)	-	-	-	2
17/03/96	50159.77	-	21.49(0.12)	21.48(0.10)	-	-	3
SN 1992A							
14/01/92	48635.06	-	12.84(0.01)	12.81(0.01)	12.76(0.01)	-	6
15/01/92	48636.06	-	12.86(0.01)	12.79(0.01)	12.75(0.01)	-	6
16/01/92	48637.03	-	12.75(0.01)	12.73(0.01)	-	-	6
17/01/92	48638.03	-	12.68(0.01)	12.69(0.01)	-	-	6
18/01/92	48639.03	-	12.62(0.01)	12.66(0.01)	12.70(0.01)	-	6
04/02/92	48656.57	-	14.17(0.01)	13.43(0.01)	13.32(0.01)	-	3
11/03/92	48692.03	-	16.03(0.03)	15.19(0.02)	15.10(0.02)	-	3
26/07/92	48829.92	-	17.94(0.03)	18.24(0.03)	18.53(0.03)	-	2
01/09/92	48867.80	-	18.43(0.03)	18.61(0.03)	19.15(0.04)	18.90(0.05)	3
30/09/92	48895.40	-	-	-	20.00(0.07)	-	5
23/10/92	48918.74	-	18.94(0.05)	19.60(0.05)	20.18(0.05)	19.69(0.08)	2
29/11/92	48956.70	-	19.69(0.08)	19.98(0.05)	20.66(0.05)	20.09(0.08)	3
02/12/92	48958.63	-	-	20.08(0.07)	-	-	6
22/12/92	48979.64	-	19.99(0.08)	20.29(0.07)	20.76(0.06)	20.16(0.07)	3
24/01/93	49011.55	-	20.43(0.08)	20.68(0.09)	21.28(0.08)	20.54(0.10)	3
24/01/93	49011.55	-	-	20.76(0.09)	21.15(0.07)	-	3
27/02/93	49045.54	-	20.74(0.10)	21.23(0.12)	-	21.10(0.15)	2
28/02/93	49046.50	-	-	21.22(0.11)	-	-	2
27/03/93	49073.54	-	21.41(0.07)	21.49(0.07)	21.82(0.07)	-	6
07/07/93	49176.20	-	>22.5	-	-	-	1
02/08/94	49566.50	-	-	25.9 (0.30)	-	-	11
04/09/96	50331.12	-	-	>27.0	-	-	11
SN 1992K							
07/04/92	48719.80	-	19.23(0.03)	18.18(0.02)	17.90(0.02)	17.51(0.02)	2
SN 1993H							
26/04/1993	49103.67	-	20.12(0.04)	19.02(0.03)	18.51(0.03)	-	3
05/05/1993	49112.90	-	-	-	18.85(0.05)	-	1
16/05/1993	49123.67	-	20.53(0.13)	19.58(0.07)	19.32(0.06)	-	1
17/05/1993	49124.63	-	20.49(0.04)	19.70(0.05)	19.46(0.04)	-	3
08/07/1993	49176.67	-	21.73(0.20)	21.04(0.10)	21.18(0.15)	-	1

Table A1.

Date	Julian Day +2,400,000	U	B	V	R	I	telescope
			SN 1993L				
05/05/93	49112.90	-	14.84(0.05)	13.97(0.03)	13.86(0.03)	-	1
16/05/93	49123.83	-	15.94(0.09)	14.60(0.04)	14.11(0.05)	-	1
16/05/93	49123.84	-	15.94(0.09)	14.60(0.04)	14.04(0.05)	-	1
17/05/93	49124.88	-	-	-	14.17(0.02)	-	3
27/05/93	49134.40	-	16.75(0.04)	15.23(0.01)	14.87(0.02)	14.51(0.01)	6
30/05/93	49137.40	-	-	15.30(0.01)	14.79(0.02)	-	6
14/06/93	49152.70	-	16.89(0.07)	15.81(0.03)	15.44(0.03)	-	5
21/06/93	49159.70	-	16.93(0.07)	15.88(0.03)	15.60(0.04)	-	5
01/07/93	49169.43	-	17.02(0.04)	16.21(0.02)	16.05(0.02)	16.01(0.02)	6
07/07/93	49176.15	-	17.29(0.10)	16.42(0.06)	16.29(0.05)	-	1
10/07/93	49178.40	-	17.31(0.04)	16.52(0.02)	16.35(0.02)	16.32(0.03)	3
11/07/93	49179.40	-	17.30(0.04)	16.56(0.02)	16.41(0.03)	16.34(0.03)	3
13/07/93	49181.40	-	17.38(0.04)	16.59(0.02)	16.44(0.03)	16.45(0.03)	3
23/08/93	49223.84	-	17.81(0.05)	17.55(0.03)	17.68(0.04)	-	3
10/09/93	49241.70	19.40(0.09)	18.22(0.09)	18.00(0.05)	18.19(0.05)	18.19(0.05)	5
18/11/93	49309.52	-	19.05(0.12)	19.06(0.06)	19.36(0.06)	19.16(0.07)	5
13/12/94	49332.57	-	-	19.70(0.07)	20.06(0.07)	-	5
15/12/94	49336.54	-	-	19.93(0.06)	19.92(0.05)	-	3
14/01/94	49367.45	-	19.64(0.09)	20.26(0.10)	-	-	3
06/05/94	49478.67	-	21.49(0.20)	-	-	-	5
09/05/94	49481.83	-	21.38(0.15)	21.51(0.10)	-	-	3
14/05/94	49486.85	-	21.45(0.20)	21.52(0.20)	-	-	2
04/06/94	49507.79	-	21.73(0.22)	21.73(0.12)	-	-	3
06/06/94	49509.88	-	21.72(0.20)	21.94(0.30)	21.70(0.20)	-	2
07/09/94	49602.63	-	22.45(0.40)	22.47(0.40)	-	-	5
07/09/94	49602.63	-	-	-	>21.91	>21.3	5
08/09/94	49603.58	-	22.88(0.40)	22.59(0.40)	-	-	5
08/09/94	49603.58	-	-	-	>22.02	>21.41	5
28/09/94	49624.67	-	23.00(0.30)	-	-	-	3
29/05/95	49866.67	-	>22.60	-	-	>21.5	6
			SN 1994D				
07/06/94	49510.54	-	15.67(0.02)	15.25(0.02)	15.14(0.02)	15.40(0.03)	3
08/06/94	49512.46	-	15.64(0.02)	15.24(0.02)	15.24(0.02)	15.44(0.03)	3
09/06/94	49513.46	-	-	15.35(0.02)	15.34(0.02)	-	3
13/06/94	49516.51	16.25(0.02)	15.75(0.01)	15.43(0.01)	15.42(0.01)	15.58(0.01)	2
14/06/94	49517.60	-	-	-	15.47(0.01)	-	2
25/06/94	49529.47	-	15.99(0.03)	15.69(0.03)	15.79(0.03)	16.12(0.03)	5
13/07/94	49546.51	-	16.26(0.03)	16.14(0.04)	16.20(0.03)	16.59(0.04)	5
08/01/95	49725.78	-	18.62(0.04)	19.03(0.04)	-	-	3
28/01/95	49745.85	-	19.11(0.09)	19.47(0.06)	-	-	5
04/02/95	49752.85	-	19.07(0.03)	-	-	-	2
05/02/95	49753.79	-	19.03(0.03)	19.60(0.02)	-	-	2
20/02/95	49768.87	-	19.46(0.10)	19.97(0.10)	-	-	1
27/02/95	49776.30	-	19.75(0.08)	-	-	-	6
28/02/95	49776.46	-	19.79(0.15)	-	-	-	7
24/04/95	49831.67	-	20.56(0.14)	-	-	-	5
24/04/95	49831.67	-	-	>20.50	-	-	5
28/05/95	49865.67	-	20.91(0.20)	-	-	-	6
28/05/95	49865.67	-	-	>20.54	-	-	6
			SN 1994M				
14/05/94	49486.56	-	17.28(0.01)	16.84(0.01)	16.83(0.01)	17.25(0.01)	2

Table A1.

Date	Julian Day +2,400,000	U	B	V	R	I	telescope
			SN 1994ae				
23/12/94	49709.85	-	15.02(0.05)	14.20(0.03)	13.94(0.03)	13.96(0.03)	1
13/01/95	49730.33	-	16.14(0.01)	15.17(0.01)	14.89(0.01)	14.67(0.01)	4
28/01/95	49745.77	-	16.34(0.04)	15.60(0.03)	15.40(0.03)	15.33(0.03)	5
05/02/95	49753.70	-	16.53(0.02)	15.83(0.02)	15.74(0.02)	15.71(0.02)	2
20/02/95	49768.79	-	16.69(0.05)	16.20(0.05)	16.12(0.05)	16.18(0.04)	1
27/02/95	49776.27	-	-	16.38(0.02)	-	-	6
27/02/95	49775.46	-	16.90(0.07)	16.28(0.05)	16.26(0.05)	16.56(0.04)	7
28/02/95	49776.46	-	16.90(0.07)	16.30(0.05)	16.37(0.06)	16.63(0.05)	7
31/03/95	49807.54	-	-	-	-	17.35(0.04)	3
20/04/95	49827.68	-	-	17.39(0.07)	17.63(0.07	18.00(0.06)	1
24/04/95	49831.67	-	17.80(0.06)	17.77(0.05)	17.89(0.05)	-	5
29/05/95	49866.67	-	18.46(0.07)	18.39(0.07)	18.82(0.05)	-	6
19/01/96	50101.77	-	21.45(0.20)	21.65(0.15)	-	-	2
21/02/96	50135.67	-	21.89(0.30)	22.09(0.17)	-	-	5
13/05/96	50216.67	-	>22.70	>22.80	-	-	5
			SN 1995D				
20/02/95	49768.78	-	13.39(0.01)	13.44(0.01)	13.47(0.02)	13.68(0.03)	1
27/02/95	49776.30	-	-	13.64(0.01)	13.75(0.01)	-	6
30/03/95	49806.59	-	-	15.24(0.01)	-	-	3
19/04/95	49827.68	-	16.74(0.12)	15.82(0.10)	15.64(0.10)	15.59(0.10)	1
25/04/95	49831.67	-	16.80(0.12)	15.97(0.11)	15.93(0.10)	15.71(0.10)	5
29/05/95	49867.67	-	17.40(0.06)	16.87(0.06)	16.88(0.04)	17.10(0.05)	6
22/11/95	50044.62	-	19.86(0.15)	20.13(0.10)	-	-	7
23/11/95	50045.58	-	19.65(0.14)	-	-	-	7
25/12/95	50077.85	-	20.08(0.10)	20.48(0.10)	-	-	2
19/01/96	50101.67	-	20.79(0.22)	20.84(0.12)	21.69(0.15)	21.10(0.20)	5
01/02/96	50114.67	-	21.11(0.09)	21.50(0.08)	-	-	1
01/02/96	50114.67	-	-	21.32(0.08)	-	-	1
15/02/96	50128.56	-	21.13(0.20)	21.24(0.20)	-	-	7
16/02/96	50129.60	-	-	-	22.26(0.30)	-	7
16/02/96	50129.57	-	-	21.24(0.20)	-	-	7
18/02/96	50131.68	-	20.86(0.25)	21.27(0.10)	22.12(0.10)	-	2
21/02/96	50134.67	-	21.31(0.30)	21.36(0.15)	22.15(0.20)	21.04(0.10)	5
19/04/96	50192.67	-	22.16(0.50)	22.30(0.22)	23.39(0.50)	-	5
10/02/97	50489.67	-	-	>23.0	-	-	3
			SN 1995ac				
02/10/95	49992.67	-	17.24(0.02)	17.26(0.02)	17.19(0.02)	17.32(0.02)	3
13/10/95	50004.64	-	17.93(0.15)	17.53(0.06)	17.50(0.06)	17.79(0.15)	3
14/11/95	50035.67	-	20.25(0.08)	19.19(0.07)	18.59(0.06)	18.47(0.07)	6
09/06/96	50243.83	-	>23.49	22.79(0.20)	-	-	3
			SN 1995bd				
18/01/96	50100.67	-	18.19(0.01)	17.12(0.01)	-	-	2
			SN 1996bo				
24/10/96	50380.65	-	16.33(0.03)	16.05(0.03)	15.79(0.03)	-	5
19/11/96	50406.64	18.46(0.08	17.81(0.08)	16.60(0.04)	16.21(0.03)	16.09(0.04)	5

Table A1.

Date	Julian Day +2,400,000	U	B	V	R	I	telescope
			SN 1997bp				
08/04/97	50547.49	-	14.19(0.02)	14.02(0.02)	13.91(0.02)	-	7
17/04/97	50555.73	14.92(0.04)	14.47(0.04)	14.01(0.03)	13.99(0.03)	14.47(0.03)	5
18/04/97	50556.68	15.06(0.04)	14.54(0.04)	14.01(0.03)	14.01(0.03)	14.50(0.03)	5
19/04/97	50557.65	15.10(0.05)	14.64(0.05)	14.12(0.03)	14.12(0.03)	14.62(0.03)	5
26/04/97	50565.74	16.06(0.06)	15.47(0.05)	14.58(0.03)	14.43(0.03)	14.81(0.03)	5
13/05/97	50581.67	-	16.93(0.01)	15.43(0.01)	14.93(0.01)	14.59(0.01)	2
02/01/98	50815.88	-	20.11(0.14)	20.07(0.08)	20.79(0.09)	20.44(0.09)	5
02/02/98	50846.81	-	20.66(0.15)	20.65(0.10)	-	-	8
26/03/98	50898.75	-	-	-	21.85(0.20)	-	5
29/05/98	50962.64	-	22.17(0.20)	22.16(0.15)	-	-	8
			SN 1997br				
17/04/97	50555.75	13.58(0.03)	14.18(0.03)	13.93(0.03)	13.74(0.03)	13.65(0.03)	5
19/04/97	50557.66	13.64(0.03)	14.13(0.03)	13.87(0.03)	13.70(0.03)	13.62(0.03)	5
13/05/97	50581.77	-	16.03(0.01)	14.64(0.01)	14.25(0.01)	-	2
09/08/97	50670.38	-	-	-	17.24(0.05)	-	1
22/03/98	50894.79	-	21.26(0.18)	21.06(0.15)	21.63(0.17)	-	1
29/05/98	50962.67	-	21.94(0.20)	21.82(0.15)	22.04(0.19)	-	8
			SN 1999aa				
16/03/99	51254.67	16.86(0.07)	16.51(0.06)	15.76(0.02)	15.66(0.03)	15.86(0.04)	5
17/03/99	51255.57	16.91(0.07)	16.61(0.06)	15.80(0.03)	15.67(0.03)	15.84(0.04)	5
12/04/99	51281.46	18.27(0.05)	17.98(0.05)	17.10(0.04)	16.80(0.04)	16.73(0.05)	8
			SN 1999dk				
25/08/99	51415.67	14.94(0.07)	15.06(0.05)	14.93(0.04)	14.92(0.04)	15.30(0.04)	1
02/09/99	51423.67	15.62(0.07)	15.45(0.06)	15.14(0.04)	15.23(0.05)	15.78(0.05)	1
05/09/99	51426.67	16.12(0.08)	15.82(0.07)	15.38(0.04)	15.49(0.05)	15.95(0.05)	1
14/09/99	51435.78	17.24(0.15)	16.75(0.05)	15.85(0.03)	15.68(0.03)	15.92(0.03)	8
17/09/99	51438.67	17.54(0.20)	17.11(0.05)	16.01(0.03)	15.70(0.03)	15.80(0.03)	8
08/10/99	51459.56	19.10(0.15)	18.12(0.03)	16.63(0.03)	16.58(0.02)	16.63(0.02)	9
			SN 2000cx				
27/07/00	51753.90	-	13.44(0.02)	13.24(0.03)	13.35(0.03)	13.77(0.02)	6
18/11/00	51866.55	18.31(0.02)	17.86(0.01)	17.76(0.01)	17.80(0.02)	18.21(0.02)	1

APPENDIX B: SNe DATA

Table B1: (1) the SN name; (2) the apparent B magnitude at maximum; (3) the stretch factor (s^{-1}) and (4) the $\Delta m_{15}(B)_{obs}$ measured as explained in §2.1, not corrected for colour excess; (5) the Galactic colour excess $E(B-V)_{gal}$ from Schlegel et al. (1998); (6) the colour excess at the blue maximum $E(B-V)_{max}$ corrected for galactic extinction; (7) the colour excess measured in the tail: $E(B-V)_{tail}$, corrected for galactic extinction; (8) the weighted mean of $E(B-V)_{max}$ and $E(B-V)_{tail}$: $E(B-V)_{host}$. $E(B-V)_{host} = E(B-V)_{tail}$ when $E(B-V)_{max}$ it is not available; (9) distance modulus μ from the Nearby Galaxy Catalogue (Tully 1988); (10) the recession velocity v_{3k} with respect to the microwave background from NED. The data sources are reported in Table B2.

Table B1.

SN (1)	m(B) (2)	s^{-1} (3)	$\Delta m_{15}(B)_{obs}$ (4)	$E(B-V)_{gal}$ (5)	$E(B-V)_{max}$ (6)	$E(B-V)_{tail}$ (7)	$E(B-V)_{host}$ (8)	μ_{tully} (9)	v_{3k} (10)
1937C	8.94(0.30)	-	0.85(0.10)	0.014	0.08(0.20)	0.06(0.05)	0.06(0.05)	28.22	543
1972E	8.40(0.04)	0.96(0.06)	1.05(0.05)	0.056	-0.04(0.10)	0.03(0.05)	0.01(0.05)	27.53	671
1972J	14.80(0.20)	1.22(0.09)	1.45(0.20)	0.046	-0.05(0.11)	0.00(0.20)	0.00(0.05)	-	2865
1974G	12.34(0.04)	1.14(0.08)	1.40(0.04)	0.019	0.25(0.20)	0.25(0.20)	0.25(0.05)	29.93	992
1980N	12.49(0.04)	1.06(0.07)	1.30(0.05)	0.021	0.05(0.06)	0.12(0.05)	0.09(0.05)	31.14	1678
1981B	12.04(0.04)	1.10(0.07)	1.13(0.05)	0.018	0.12(0.06)	0.10(0.14)	0.11(0.05)	-	2141
1982B	13.65(0.20)	-	0.94(0.10)	0.064	-	0.14(0.14)	0.14(0.14)	32.68	2203
1983G	13.00(0.10)	1.18(0.08)	1.30(0.20)	0.034	0.19(0.11)	0.42(0.05)	0.35(0.16)	30.89	1566
1986G	12.48(0.04)	1.37(0.11)	1.69(0.05)	0.115	0.95(0.08)	0.67(0.05)	0.78(0.20)	28.45	806
1989B	12.38(0.12)	1.04(0.07)	1.28(0.05)	0.032	0.41(0.06)	0.46(0.14)	0.42(0.05)	29.10	1067
1990N	12.75(0.04)	1.04(0.07)	1.05(0.05)	0.026	0.09(0.06)	0.18(0.05)	0.14(0.06)	31.13	1322
1990O	16.59(0.04)	0.91(0.08)	0.94(0.05)	0.093	0.05(0.10)	0.10(0.05)	0.08(0.05)	-	9175
1990T	17.27(0.20)	-	1.13(0.20)	0.053	0.08(0.30)	0.16(0.05)	0.15(0.06)	-	11893
1990Y	17.69(0.20)	-	1.13(0.20)	0.008	0.26(0.30)	0.34(0.10)	0.32(0.05)	-	11652
1991S	17.78(0.05)	-	1.00(0.10)	0.026	0.06(0.30)	0.13(0.10)	0.11(0.05)	-	16807
1991T	11.69(0.04)	0.93(0.05)	0.94(0.05)	0.022	0.21(0.06)	0.19(0.04)	0.20(0.05)	30.65	2070
1991U	16.67(0.10)	-	1.11(0.10)	0.062	0.07(0.30)	0.15(0.20)	0.12(0.05)	-	9724
1991ag	14.67(0.04)	0.89(0.02)	0.87(0.05)	0.062	0.06(0.30)	0.08(0.05)	0.08(0.05)	-	4521
1991bg	14.75(0.04)	1.47(0.22)	1.94(0.05)	0.041	-0.00(0.07)	0.00(0.09)	0.00(0.05)	31.13	1282
1992A	12.56(0.04)	1.25(0.09)	1.47(0.05)	0.018	0.05(0.07)	0.02(0.05)	0.04(0.05)	31.14	1737
1992J	17.88(0.20)	-	1.69(0.20)	0.057	-	0.10(0.08)	0.10(0.08)	-	13828
1992K	16.31(0.20)	-	1.94(0.20)	0.101	-	0.00(0.05)	0.00(0.05)	-	3324
1992P	16.14(0.20)	1.00(0.03)	1.05(0.30)	0.021	0.05(0.06)	0.12(0.05)	0.09(0.05)	-	7939
1992ae	18.62(0.04)	-	1.30(0.10)	0.036	0.12(0.11)	0.05(0.10)	0.09(0.05)	-	22442
1992ag	16.64(0.20)	1.07(0.07)	1.20(0.20)	0.097	0.15(0.06)	0.45(0.20)	0.22(0.21)	-	8095
1992al	14.59(0.04)	1.00(0.03)	1.09(0.05)	0.034	-0.01(0.06)	0.07(0.04)	0.04(0.05)	-	4214
1992aq	19.42(0.10)	-	1.69(0.05)	0.012	0.05(0.31)	0.00(0.20)	0.02(0.05)	-	30014
1992au	18.17(0.20)	-	1.69(0.30)	0.017	-	0.00(0.30)	0.00(0.30)	-	18225
1992bc	15.13(0.04)	0.93(0.05)	0.90(0.05)	0.022	0.01(0.06)	-0.03(0.05)	0.00(0.05)	-	5876
1992bg	17.39(0.04)	1.00(0.03)	1.15(0.05)	0.185	-0.04(0.20)	0.04(0.05)	0.02(0.06)	-	10936
1992bh	17.68(0.04)	0.98(0.03)	1.13(0.05)	0.022	0.10(0.10)	0.13(0.10)	0.12(0.05)	-	13519
1992bk	18.07(0.04)	-	1.67(0.05)	0.015	0.04(0.21)	-0.01(0.10)	0.01(0.05)	-	17551
1992bl	17.34(0.04)	1.23(0.05)	1.56(0.05)	0.011	-0.02(0.11)	0.04(0.05)	0.02(0.05)	-	12661
1992bo	15.86(0.04)	1.33(0.11)	1.69(0.05)	0.027	-0.02(0.08)	-0.01(0.12)	0.00(0.05)	-	5164
1992bp	18.53(0.04)	1.12(0.04)	1.52(0.20)	0.069	-0.02(0.11)	0.00(0.20)	0.00(0.05)	-	23557
1992bs	18.33(0.04)	1.01(0.03)	1.15(0.05)	0.011	0.06(0.10)	0.05(0.10)	0.05(0.05)	-	18787
1993B	18.71(0.06)	0.99(0.03)	1.30(0.05)	0.079	-0.02(0.20)	0.24(0.10)	0.15(0.18)	-	21011
1993H	16.99(0.04)	1.18(0.04)	1.69(0.10)	0.060	0.16(0.08)	0.06(0.05)	0.10(0.07)	-	7523
1993L	13.40(0.20)	-	1.47(0.30)	0.014	0.31(0.21)	0.32(0.11)	0.32(0.05)	-	1387
1993O	17.79(0.04)	1.05(0.07)	1.26(0.05)	0.053	-0.07(0.06)	0.04(0.08)	0.00(0.08)	-	15867
1993ac	18.45(0.20)	-	1.25(0.20)	0.163	-	0.04(0.10)	0.04(0.10)	-	14674
1993ae	15.44(0.20)	-	1.47(0.20)	0.038	-0.01(0.30)	0.00(0.05)	0.00(0.05)	-	5405
1993ag	18.30(0.04)	1.06(0.03)	1.30(0.20)	0.112	0.15(0.06)	0.10(0.10)	0.13(0.05)	-	15031
1993ah	16.32(0.04)	1.19(0.14)	1.45(0.10)	0.020	-	0.15(0.10)	0.15(0.10)	-	8604
1994D	11.86(0.04)	1.27(0.10)	1.31(0.05)	0.022	-0.02(0.06)	0.05(0.08)	0.01(0.05)	31.13	793
1994M	16.35(0.06)	1.18(0.04)	1.45(0.20)	0.023	0.12(0.11)	0.18(0.05)	0.16(0.05)	-	7289
1994Q	16.44(0.10)	-	0.90(0.10)	0.017	-	0.11(0.06)	0.11(0.06)	-	8954

Table B1.

SN (1)	m(B) (2)	s^{-1} (3)	$\Delta m_{15}(B)_{obs}$ (4)	$E(B-V)_{gal}$ (5)	$E(B-V)_{max}$ (6)	$E(B-V)_{tail}$ (7)	$E(B-V)_{host}$ (8)	μ_{tully} (9)	v_{3k} (10)
1994T	17.23(0.10)	-	1.45(0.05)	0.029	0.06(0.30)	0.07(0.20)	0.07(0.05)	-	10708
1994ae	13.15(0.06)	1.04(0.07)	0.87(0.10)	0.030	0.17(0.06)	0.16(0.09)	0.16(0.05)	31.85	1609
1995D	13.44(0.04)	0.99(0.06)	1.03(0.05)	0.058	0.07(0.06)	0.13(0.07)	0.10(0.05)	32.43	2289
1995E	16.82(0.04)	0.96(0.03)	1.19(0.05)	0.027	0.77(0.06)	0.72(0.14)	0.76(0.05)	-	3510
1995ac	17.21(0.04)	0.96(0.06)	0.95(0.05)	0.042	0.06(0.06)	-0.01(0.05)	0.02(0.05)	-	14635
1995ak	16.09(0.10)	1.11(0.07)	1.45(0.10)	0.038	-0.04(0.11)	0.28(0.06)	0.16(0.23)	-	6589
1995al	13.36(0.04)	0.93(0.03)	0.89(0.05)	0.014	0.21(0.06)	0.19(0.05)	0.20(0.05)	32.00	1797
1995bd	17.27(0.04)	0.93(0.05)	0.88(0.05)	0.498	0.37(0.06)	0.20(0.05)	0.28(0.12)	-	4326
1996C	16.59(0.08)	0.87(0.02)	0.94(0.10)	0.013	0.11(0.20)	0.07(0.05)	0.08(0.05)	-	8245
1996X	13.26(0.04)	1.09(0.07)	1.32(0.05)	0.069	-0.00(0.06)	0.07(0.07)	0.03(0.05)	32.29	2325
1996ai	16.96(0.20)	0.83(0.02)	0.85(0.08)	0.014	1.76(0.06)	2.07(0.10)	1.88(0.22)	31.64	1177
1996bk	14.84(0.20)	-	1.69(0.20)	0.018	0.38(0.21)	0.33(0.13)	0.35(0.05)	32.55	2147
1996bl	17.08(0.04)	0.99(0.03)	1.11(0.05)	0.092	0.05(0.06)	0.13(0.07)	0.09(0.05)	-	10447
1996bo	16.15(0.04)	1.06(0.07)	1.30(0.05)	0.077	0.35(0.06)	0.30(0.10)	0.33(0.05)	-	4898
1996bv	15.77(0.04)	-	0.84(0.10)	0.105	0.23(0.20)	0.23(0.10)	0.23(0.05)	-	5016
1997bp	14.10(0.20)	0.95(0.09)	0.94(0.20)	0.044	0.09(0.20)	0.45(0.20)	0.27(0.26)	-	2824
1997br	14.06(0.04)	1.04(0.07)	1.04(0.05)	0.113	0.31(0.20)	0.33(0.04)	0.33(0.05)	-	2399
1998bu	12.20(0.04)	1.00(0.06)	1.15(0.05)	0.025	0.39(0.06)	0.36(0.05)	0.37(0.05)	29.54	1238
1998de	17.56(0.02)	1.45(0.13)	1.94(0.05)	0.059	-0.08(0.07)	0.00(0.10)	0.00(0.05)	-	4713
1999aa	14.93(0.05)	0.85(0.07)	0.85(0.05)	0.040	0.11(0.06)	0.07(0.05)	0.09(0.05)	-	4564
1999aw	16.86(0.05)	0.74(0.05)	0.81(0.05)	0.032	0.10(0.09)	0.00(0.10)	0.05(0.07)	-	11362
1999da	16.90(0.10)	-	1.94(0.20)	0.058	-	0.05(0.20)	0.05(0.20)	-	3644
1999dk	15.04(0.05)	0.92(0.08)	1.28(0.10)	0.054	0.13(0.06)	0.17(0.21)	0.14(0.05)	-	4184
1999ee	14.94(0.02)	0.86(0.04)	0.92(0.05)	0.020	0.36(0.06)	0.39(0.06)	0.38(0.05)	-	3153
1999gp	16.25(0.05)	0.83(0.07)	0.94(0.10)	0.056	0.15(0.06)	0.11(0.09)	0.14(0.05)	-	7811
2000E	14.31(0.05)	0.85(0.07)	0.94(0.05)	0.366	0.21(0.10)	0.30(0.10)	0.25(0.07)	31.91	1280
2000bk	16.98(0.10)	1.32(0.17)	1.69(0.10)	0.025	-	0.19(0.05)	0.19(0.05)	-	7976
2000ce	17.24(0.10)	0.86(0.07)	0.94(0.10)	0.057	-	0.65(0.14)	0.65(0.14)	-	4948
2000cx	13.44(0.05)	0.94(0.09)	0.93(0.05)	0.083	0.19(0.06)	-0.20(0.05)	0.00(0.28)	32.53	2115
2001el	12.81(0.02)	1.02(0.06)	1.15(0.05)	0.014	0.13(0.06)	0.33(0.05)	0.24(0.14)	30.55	1091
2002bo	14.01(0.10)	1.02(0.06)	1.17(0.05)	0.025	0.48(0.06)	0.47(0.05)	0.47(0.05)	31.76	1641

Table B2.

SN	References	SN	References
1937C	B.E. Schaefer, 1994, ApJ, 426, 493	1983G	W. E. Harris et al., 1983, PASP, 95, 607
	M.J. Pierce & G.H. Jacoby, 1995, AJ, 110, 2885		R.J. Buta et al., 1985, PASP, 97, 229
1972E	A. Ardeberg & M. de Groot, 1973, A&A, 28, 295		S. Benetti et al., 1991, A&A, 247, 410
	A.M. van Genderen, 1975, A&A, 45, 429		D.Y. Tsvetkov, 1985, SA, 29, 211
	T.A. Lee et al., 1972, ApJ, 177, L59	1986G	M.M. Phillips et al., 1987, PASP, 99, 592
	A.W.J. Cousins 1972, IBVS, 700, 1		S. Cristiani et al., 1992, A&A, 259, 63
1972J	F. Ciatti & L. Rosino, 1977, A&A 57, 73 *		B.E. Schaefer 1987, ApJ, 323, 47
	* revised in F. Patat et al. 1997 A&A, 317, 423	1989B	R. Barbon et al., 1990, A&A, 237, 79
1974G	F. Ciatti & L. Rosino, 1977, A&A 57, 73		L.A. Wells et al., 1994, AJ, 108, 2233
	B. Patchett & R. Wood, 1976, MNRAS, 175, 595	1990N	P. Lira et al., 1998, AJ, 115, 234
	I.D. Howarth, 1974, Mitt. Veränderl Sterne, 6, 155	1990O	M. Hamuy et al., 1996, AJ, 112, 2408
1980N	M. Hamuy et al., 1991, AJ, 102, 208	1990T	M. Hamuy et al., 1996, AJ, 112, 2408
	P.F. Younger & S. van den Bergh, 1985, A&AS, 61, 365	1990Y	M. Hamuy et al., 1996, AJ, 112, 2408
1981B	R. Barbon; F. Ciatti; L. Rosino, 1982, A&A, 116, 35 *	1991S	M. Hamuy et al., 1996, AJ, 112, 2408
	* revised in F. Patat et al. 1997 A&A, 317, 423		ESO-Asiago SN Archive
	R.J. Buta & A. Turner, 1983, PASP, 95, 72	1991T	P. Lira et al., 1998, AJ, 115, 234
	D.Y. Tsvetkov, 1982, SA, 8, 115		E. Cappellaro et al., 1997, A&A, 328, 203
	IAUC 3584		B. Schmidt et al., 1994 ApJ, 434, 19
1982B	D.Y. Tsvetkov, 1986, PZ, 22, 279		IAUC 5246, 5253, 5256, 5270, 5273, 5309
	F. Ciatti et al., 1988, A&A, 202, 15		W.B. Sparks et al., 1999, ApJ, 523, 585
	R. Cadanau & C., Trefzger, 1983, IBVS, 2382, 1	1991U	M. Hamuy et al., 1996, AJ, 112, 2408

Table B2.

SN	References
1991ag	M. Hamuy et al., 1996, AJ, 112, 2408
1991bg	B. Leibundgut et al., 1993, AJ, 105, 301
	A.V. Filippenko et al., 1992, AJ, 104, 1543
	M. Turatto et al., 1996, MNRAS, 283, 1
1992A	N.B Suntzeff, 1996, in McCray Z. Wang (eds.), Supernovae and Supernova Remnants, p.41, Cambridge Univ. Press, Cambridge
	E. Cappellaro et al., 1997, A&A, 328, 203
1992J	M. Hamuy et al., 1996, AJ, 112, 2408
1992K	ESO-Asiago SN Archive
	M. Hamuy et al., 1996, AJ, 112, 2408
1992P	M. Hamuy et al., 1996, AJ, 112, 2408
1992ae	M. Hamuy et al., 1996, AJ, 112, 2408
1992ag	M. Hamuy et al., 1996, AJ, 112, 2408
1992al	M. Hamuy et al., 1996, AJ, 112, 2408
1992aq	M. Hamuy et al., 1996, AJ, 112, 2408
1992au	M. Hamuy et al., 1996, AJ, 112, 2408
1992bc	M. Hamuy et al., 1996, AJ, 112, 2408
1992bg	M. Hamuy et al., 1996, AJ, 112, 2408
1992bh	M. Hamuy et al., 1996, AJ, 112, 2408
1992bk	M. Hamuy et al., 1996, AJ, 112, 2408
1992bl	M. Hamuy et al., 1996, AJ, 112, 2408
1992bo	M. Hamuy et al., 1996, AJ, 112, 2408
1992bp	M. Hamuy et al., 1996, AJ, 112, 2408
1992bs	M. Hamuy et al., 1996, AJ, 112, 2408
1993B	M. Hamuy et al., 1996, AJ, 112, 2408
1993H	M. Hamuy et al., 1996, AJ, 112, 2408
	IAUC 5723
	ESO-Asiago SN Archive
1993L	IAUC 5780, 5781
	E. Cappellaro et al., 1997, A&A, 328, 203
1993O	M. Hamuy et al., 1996, AJ, 112, 2408
1993ac	A.G. Riess et al., 1999, AJ, 117, 707
1993ae	A.G. Riess et al., 1999, AJ, 117, 707
	W.C.G. Ho et al., 2001, PASP, 113, 1349
1993ag	M. Hamuy et al., 1996, AJ, 112, 2408
1993ah	M. Hamuy et al., 1996, AJ, 112, 2408
1994D	F. Patat et al., 1996, MNRAS, 278, 111
	E. Cappellaro et al., 1997, A&A, 328, 203
	S. D. Van Dyk et al., 1999, AJ, 118, 2331
	M.W. Richmond et al., 1995, AJ 109, 2121
	W.P.S. Meikle et al., 1996, MNRAS, 281, 263
	D.Y. Tsvetkov & N.N. Pavlyuk, 1995, AstL, 21, 606
	H. Wu, H.J. Yan, Z.L. Zou, 1995, A&A, 294, 9
	M.W. Richmond et al., 1995, AJ, 109, 2121
1994M	A.G. Riess et al., 1999, AJ, 117, 707
	W.C.G. Ho et al., 2001, PASP, 113, 1349
	ESO-Asiago SN Archive
1994Q	A.G. Riess et al., 1999, AJ, 117, 707
	W.C.G. Ho et al., 2001, PASP, 113, 1349
1994T	A.G. Riess et al., 1999, AJ, 117, 707
1994ae	IAUC 6105,6111
	A.G. Riess et al., 1999, AJ, 117, 707
	ESO-Asiago SN Archive
	W.C.G. Ho et al., 2001, PASP, 113, 1349
	D.Y. Tsvetkov et al., 1997, AstL, 23, 26
1995D	IAUC 6134,6149,6156,6166
	K. Sadakane et al., 1996, PASJ, 48, 51
	ESO-Asiago SN Archive
	A.G. Riess et al., 1999, AJ, 117, 707
1995E	A.G. Riess et al., 1999, AJ, 117, 707
1995ac	A.G. Riess et al., 1999, AJ, 117, 707
	ESO-Asiago SN Archive
1995ak	A.G. Riess et al., 1999, AJ, 117, 707
1995al	IAUC 6255,6256
	A.G. Riess et al., 1999, AJ, 117, 707
	D. Yu. Tsevtkov et al. 2001 Astr. Rep. 45, 527
1995bd	A.G. Riess et al., 1999, AJ, 117, 707
	ESO-Asiago SN Archive
1996C	A.G. Riess et al., 1999, AJ, 117, 707
1996X	IAUC 6380,6381
	M.E. Salvo et al. 2001, MNRAS 321, 254
	A.G. Riess et al., 1999, AJ, 117, 707
1996ai	A.G. Riess et al., 1999, AJ, 117, 707
1996bk	A.G. Riess et al., 1999, AJ, 117, 707
1996bl	A.G. Riess et al., 1999, AJ, 117, 707
1996bo	A.G. Riess et al., 1999, AJ, 117, 707
	D. Yu. Tsevtkov et al. 2001 Astr. Rep. 45, 527
	ESO-Asiago SN Archive
1996bv	A.G. Riess et al., 1999, AJ, 117, 707
1997bp	ESO-Asiago SN Archive
	A.G. Riess et al., 1998, ApJ, 504, 935
1997br	W.D. Li et al., 1999, AJ, 117, 2709
	ESO-Asiago SN Archive
1998bu	N.B. Suntzeff et al., 1999, AJ, 117, 1175
	S. Jha et al. 1999, ApJS, 125, 73
	E. Cappellaro et al., 2001, ApJ, 549, 215
	M. Hernandez et al., 2000, MNRAS, 319, 223
1998de	M. Modjaz et al., 2001, PASP, 113, 308
1999aa	ESO-Asiago SN Archive
	K. Krisciunas et al., 2000, ApJ, 539 ,658
1999aw	L.G. Strolger et al., 2002, AJ, 124, 2905
1999da	K. Krisciunas et al., 2001, AJ, 122, 1616
1999dk	K. Krisciunas et al., 2001, AJ, 122, 1616
	ESO-Asiago SN Archive
1999ee	M.D. Stritzinger et al., 2002, AJ, 124, 2100
1999gp	K. Krisciunas et al., 2001, AJ, 122, 1616
2000E	G. Valentini et al. astro-ph/0306391
	J. Vinkó et al., 2001, A&A, 372, 824
2000bk	K. Krisciunas et al., 2001, AJ, 122, 1616
2000ce	K. Krisciunas et al., 2001, AJ, 122, 1616
2000cx	P. Candia et al., 2003, PASP, 115, 277
	ESO-Asiago SN Archive
2001el	K. Krisciunas et al., 2003, AJ, 125, 166
2002bo	IAUC 7863
	S. Benetti et al., 2003, MNRAS accepted
	Gy.M. Szabo et al., 2003, A&A, 408, 915

APPENDIX C: B BAND TEMPLATES

Table C1. Light curve templates for different decline rates.

Δm_{15}	0.82	1.02	1.11	1.29	1.42	1.67	1.94
phase				$m(B)$			
-7	0.510	0.361	0.238	0.689	0.578	0.641	1.322
-6	0.347	0.246	0.155	0.546	0.396	0.500	1.002
-5	0.217	0.168	0.098	0.405	0.264	0.363	0.683
-4	0.125	0.107	0.062	0.274	0.166	0.238	0.400
-3	0.064	0.057	0.038	0.161	0.090	0.134	0.229
-2	0.025	0.021	0.019	0.073	0.038	0.059	0.125
-1	0.005	0.002	0.005	0.019	0.008	0.015	0.028
0	0.000	0.000	0.000	0.000	0.000	0.000	0.000
1	0.008	0.015	0.011	0.010	0.014	0.014	0.036
2	0.027	0.041	0.042	0.040	0.048	0.053	0.106
3	0.054	0.073	0.085	0.084	0.101	0.114	0.186
4	0.087	0.107	0.132	0.140	0.168	0.191	0.296
5	0.124	0.148	0.181	0.207	0.246	0.280	0.465
6	0.166	0.199	0.236	0.285	0.331	0.377	0.647
7	0.213	0.262	0.300	0.371	0.421	0.485	0.844
8	0.268	0.337	0.378	0.466	0.518	0.605	1.046
9	0.332	0.421	0.468	0.569	0.627	0.741	1.240
10	0.402	0.509	0.565	0.680	0.745	0.891	1.417
11	0.477	0.601	0.666	0.798	0.873	1.049	1.565
12	0.554	0.698	0.766	0.924	1.010	1.211	1.687
13	0.634	0.802	0.871	1.051	1.150	1.369	1.787
14	0.721	0.910	0.985	1.173	1.288	1.521	1.868
15	0.815	1.018	1.109	1.285	1.418	1.664	1.935
16	0.915	1.122	1.239	1.390	1.539	1.799	1.992
17	1.019	1.225	1.371	1.491	1.656	1.926	2.042
18	1.126	1.327	1.499	1.593	1.769	2.046	2.088
19	1.235	1.428	1.622	1.697	1.880	2.158	2.133
20	1.344	1.529	1.739	1.802	1.990	2.262	2.181
21	1.453	1.629	1.851	1.908	2.099	2.359	2.231
22	1.560	1.727	1.958	2.013	2.205	2.447	2.280
23	1.665	1.822	2.059	2.116	2.308	2.529	2.328
24	1.769	1.915	2.156	2.217	2.408	2.602	2.372
25	1.869	2.005	2.247	2.314	2.504	2.668	2.413
26	1.966	2.091	2.333	2.406	2.595	2.729	2.449
27	2.059	2.172	2.414	2.493	2.680	2.782	2.480
28	2.147	2.248	2.491	2.572	2.758	2.831	2.507
29	2.230	2.321	2.562	2.644	2.828	2.874	2.531
30	2.310	2.387	2.629	2.709	2.889	2.914	2.550
31	2.385	2.450	2.691	2.767	2.944	2.951	2.567
32	2.455	2.509	2.749	2.819	2.990	2.984	2.582
33	2.521	2.565	2.801	2.864	3.031	3.016	2.597
34	2.584	2.617	2.849	2.905	3.067	3.044	2.612
35	2.641	2.667	2.892	2.942	3.099	3.071	2.628
36	2.695	2.714	2.930	2.977	3.128	3.096	2.648
37	2.745	2.759	2.963	3.012	3.155	3.120	2.670
38	2.791	2.802	2.991	3.048	3.180	3.141	2.695
39	2.833	2.843	3.016	3.083	3.202	3.162	2.722
40	2.873	2.883	3.036	3.118	3.223	3.181	2.750
41	2.909	2.920	3.055	3.150	3.243	3.200	2.778
42	2.942	2.956	3.071	3.180	3.261	3.217	2.806
43	2.973	2.989	3.086	3.205	3.277	3.234	2.832
44	3.001	3.019	3.099	3.225	3.291	3.251	2.856
45	3.027	3.047	3.113	3.240	3.304	3.267	2.877
46	3.052	3.073	3.127	3.254	3.315	3.283	2.896
47	3.075	3.096	3.142	3.266	3.324	3.299	2.914
48	3.095	3.116	3.157	3.279	3.331	3.315	2.930
49	3.116	3.135	3.173	3.294	3.339	3.330	2.946
50	3.135	3.151	3.189	3.311	3.351	3.346	2.963
51	3.154	3.166	3.204	3.329	3.364	3.361	2.982
52	3.172	3.180	3.220	3.349	3.382	3.377	3.001
53	3.188	3.193	3.235	3.369	3.402	3.393	3.021
54	3.203	3.205	3.250	3.388	3.423	3.409	3.042
55	3.219	3.216	3.265	3.408	3.444	3.426	3.062
56	3.233	3.227	3.279	3.427	3.465	3.443	3.082
57	3.247	3.238	3.294	3.445	3.485	3.460	3.102
58	3.261	3.249	3.307	3.463	3.504	3.477	3.122
59	3.274	3.260	3.321	3.481	3.523	3.495	3.142
60	3.288	3.272	3.334	3.497	3.540	3.513	3.161
61	3.301	3.284	3.346	3.513	3.557	3.531	3.181
62	3.314	3.298	3.359	3.528	3.574	3.550	3.201
63	3.327	3.312	3.371	3.542	3.590	3.569	3.221
64	3.340	3.327	3.383	3.555	3.605	3.588	3.242
65	3.353	3.342	3.395	3.567	3.620	3.607	3.263
66	3.366	3.358	3.406	3.578	3.636	3.627	3.284
67	3.379	3.374	3.417	3.589	3.650	3.646	3.306
68	3.391	3.391	3.428	3.600	3.664	3.666	3.329
69	3.404	3.409	3.439	3.611	3.679	3.685	3.353
70	3.417	3.427	3.449	3.621	3.693	3.705	3.378
71	3.430	3.445	3.459	3.632	3.707	3.724	3.404
72	3.442	3.463	3.469	3.643	3.720	3.743	3.430
73	3.455	3.481	3.479	3.655	3.734	3.762	3.458
74	3.468	3.500	3.489	3.667	3.749	3.780	3.488
75	3.481	3.519	3.498	3.680	3.763	3.798	3.518
76	3.493	3.537	3.507	3.694	3.778	3.816	3.549
77	3.506	3.556	3.516	3.708	3.794	3.833	3.581
78	3.519	3.574	3.525	3.723	3.809	3.849	3.613
79	3.532	3.593	3.534	3.739	3.825	3.865	3.644
80	3.545	3.611	3.542	3.756	3.842	3.880	3.676